doc//CQE/stat_cum_dyn/shallow-deep/notes.tex : 11 September 2012

# Towards a Statistical Cumulus Dynamics: Two–Mode System

*COST ES0905 Document*

by

Robert Plant
Department of Meteorology, University of Reading, UK

and
Jun-Ichi Yano,
GAME/CNRM, Météo-France and CNRS, 31057 Toulouse Cedex, France

[1] *Corresponding author address:* Robert S. Plant, Meteorology Department, University of Reading, RG6 6BB, UK. E-mail: r.s.plant@reading.ac.uk

[1]

**Abstract**

Interactions between shallow and deep atmospheric convection are investigated under the framework of an energy–cycle description. This formulation provides a lucid presentation of the interactions between the two types of convection. The analysis here is considered as a step torwards a statistical cumulus dynamics.

# Contents

# 1 Introduction

As discussed in the COST ES0905 report by Yano and Plant (2011), the energy–cycle description of a convective system provides a basis for considering the statistical dynamics of convective ensembles, as well as other basic behaviours of the convective system. Under this formulation, in general, a spectrum of convective types with various characteristic depths can be considered. The focus of discussions in Yano and Plant (2011, 2012a) has been on the case with a single convective type, namely deep convection. The present report is an expansion and development of those earlier analyses, and as such we will provide only a relatively brief introduction here. Specifically, in this report we expand the discussions and analyses to the case in which two types of convection co–exist: shallow and deep.

We believe this is a useful step forwards towards a construction of statistical cumulus dynamics for an arbitrary number of types.

## 1.1 Types of convection

The problem of atmospheric moist convection is not a simple one, partly because it takes various different forms. As was emphasized in a review by Stevens (2005), "moist convection is not one, but many things". According to this review, atmospheric moist convection can be classified into three major categories. In order of increasing vertical extent these are stratocumulus, trade–wind cumulus, and deep precipitating cumulus convection. These major categories may also be considered as a series of transformations of the dominant mode of convection with an increasing supply of moisture from the surface under a horizontally homogeneous environment. Phenomenologically, such transformations are found as we move from the mid-latitudes to the warmer tropical oceans.

Here, by "horizontally homogeneous environment" we mean an idealized situation in which horizontal advection effects can be neglected. This is a useful idealization because convection is a process primarily concerned with vertical transports. In the present study, such an idealization is adopted under the framework of a zero–spatial–dimension model.

Under this idealization, when moisture supply from the surface is totally absent, a constant heat supply from the surface (the sensible heat flux) tends to produce a well-mixed convective boundary layer. As surface moisture supply is increasingly supplied to such system, above a threshold cloud is formed at the top of the boundary layer. Such cloud is typically stratiform, and the associated convection is called stratocumulus convection (*cf.*, Moeng

1998). As the surface moisture supply is further increased, there is a regime transition from stratiform clouds into "shallow" cumulus convective towers. This regime is called trade–cumulus convection (*cf.*, Riehl 1951, Betts 1997), because it is typically found over the trade–wind region in the sub-tropics. As the surface moisture supply increases still further (as we approach closer the equator), then a final regime transition occurs in which deep cumulus convection is realized, which may reach as high as the tropopause (*cf.*, Riehl and Malkus 1958, Houze and Betts 1981, Redelsperger 1997). This last transition from shallow to deep convection is considered relatively sharp, although the existence of middle–level clouds called "cumulus congestus" has been emphasized more recently (Johnson *et al.* 1999, Tung *et al.* 1999).

A major challenge in global atmospheric modelling is to represent these rich varieties of moist convection, and the transitions between them, by means of parameterizations. Currently no single unified parameterization exists, but rather each different type of convection is dealt using a different parameterization scheme. Typically, convection parameterization schemes are distinguished into shallow and deep versions in order to deal with trade and deep cumulus convection separately (*e.g.*, Tiedtke, 1989). Stratocumulus clouds are often dealt with by a boundary–layer parameterization (*e.g.*, Holtslag and Boville 1993, Lock 1998, Lock *et al.* 2000), often also in combination with microphysics and stratiform cloud schemes (*cf.*, Wyant *et al.* 2007). The combination of these independently–developed schemes often causes a problem in simulating stratocumulus convection (*cf.*, Köller *et al.* 2011) and shallow/deep transitions (*e.g.*, Guichard *et al.* 2004).

A recent trend has seen some attempts to use a combination of eddy diffusion and mass flux approaches (*e.g.*, Neggers *et al.* 2009, Köller *et al.* 2011), especially for dealing with stratiform convection consistently with the other types of convection. Other significant recent efforts include attempts to generalize shallow–convection mass–flux parameterizations for deep convection (Hohenegger and Bretherton 2011, Mapes and Meale 2011).

## 1.2 Truncation to two types

The present report proposes to consider all types of convection by taking an energy–cycle description for a spectrum of types under a mass–flux formulation. The spectral approach, originally developed by Arakawa and Schubert (1974), treats different convection types by different prescribed vertical structures. Although Arakawa and Schubert (1974) more specifically assumed an ensemble of entraining plumes in defining their vertical structures, we do not consider this as an essential feature of their formulation because

other models for defining the vertical mass flux structure could straightforwardly be incorporated into the general framework, as discussed in Yano and Plant (2011).

Note that these various types of convection can loosely be categorized into two major types: "non-precipitating" shallow convection and precipitating deep convection. In doing so, we effectively consider stratocumulus and trade–cumulus convection together as being the first major type. Thus, in the present report, we truncate a spectral representation of convection into only two modes: shallow and deep convection. The main reason for such a severe truncation is in order elucidate the interactions between convection types in the simplest possible setting.

In the above, we added quotation marks to "non-precipitating" because shallow convection is rarely non-precipitating in a strict sense, although the precipitation is much weaker than that typical of deep convection. In fact, from the energy-cycle perspective, the fundamental separation between the two types is not whether the clouds are shallow or deep, but rather whether or not the precipiation is strong enough to alter the character of the thermodynamic budget. The key aspect is that the budgets for the two major convective types are qualitatively different.

In the shallow–convection regime, the main effects of convection on its environment are cooling and moistening. These tendencies are usually balanced by large–scale subsidence that warms and dries the environment. It is important to recognize that in the absence of such subsidence then the shallow–convectives regime is self–destabilizing. Note that shallow convection moistens the environment because it is either non-precipitating or only weakly precipitating, and thus the condensed water must ultimately return to the environment. The condensed water typically evaporates as soon as it detrains into the environment, leading to cooling as a result.

On the other hand, in the deep–convective regime, the main effects of convection on its environment are warming and drying. These tendencies are usually balanced by a large–scale ascent that cools and moistens the environment. It is important to recognize that in the absence of such ascent the deep–convective regime is self–stabilizing. Note that deep convection dries the environment because condensation within deep convection acts as a sink for moisture, which mostly returns to the surface by precipitation. The detrained dry air from deep convection must descend towards the surface as a return flow, associated with adiabatic warming.

The purpose of the present report is twofold. First, we will show that these two qualitatively different behaviours of convection can be easily incorporated and well described using an energy cycle. Second, we will show

that the energy cycle formulation can describe the interactions between shallow and deep convection. We emphasize that this aspect is somewhat neglected in current operational modelling configurations. We will systematically investigate the behaviour of the coupled shallow–deep convective system, pointing out the importance of these interactions for operational modelling contexts.

Note that the majority of the following investigation assumes no large–scale forcing. This drastic simplification enables us to examine the behaviour of the system analytically in the most lucid manner without additional complications.

## 2 Rationale

This section recalls some key ideas behind the energy–cycle formulation for the convective system originally introduced by Arakawa and Schubert (1974). More complete discussion can be found in Yano and Plant (2011) but a brief overview is provided here in order to make the presentation self-contained. The reader should bear in mind particularly that although in the following we often call a convective type a plume for convenience, the convective types need not necessarily be defined by any particular plume model, but rather the types are distinguished by vertical profiles fixed with time, whatever rule is invoked to determine the profiles.

Consider a system of $N$ plume types and let the subscripts refer to the plume types. The convective kinetic energy $K_i$ for type $i$ evolves according to the following equation (Yano and Plant 2011):

$$\frac{dK_i}{dt} = A_i M_{bi} - D_i \tag{1}$$

Thus, kinetic energy is generated from potential energy at a rate $A_i M_{bi}$, and dissipated at a rate $D_i$. The generation rate is proportional to the cloud-base mass flux $M_{bi}$ and to the cloud work function $A_i$, which itself evolves as

$$\frac{dA_i}{dt} = F_i + \sum_j \mathcal{K}_{ij} M_{bj} \tag{2}$$

Here $F_i$ is the large-scale forcing (radiative or advective tropospheric cooling, surface fluxes, etc) for convection. The action of convection itself on the cloud work function is described by the matrix $\mathcal{K}_{ij}$.

The two dominant physical processes described by the matrix $\mathcal{K}_{ij}$ are discussed in two paragraphs following Eq.(144) of Arakawa and Schubert

(1974). The most dominant process (see their Fig. 11) is adiabatic warming due to the compensative descent, $-M_j$, induced by a given convective plume $j$. This process reduces the cloud work function of all plume types. Mathematically, an important consequence to recognize is that the interaction matrix cannot be treated as sparse: in other words, all cloud types influence all other cloud types. The second major process (cf., their Fig. 12) is cooling of the environment due to re–evaporation of detrained condensed (cloudy) air. This process increases the cloud work function due to its destabilizing tendency, but it affects only the plumes of the same type or those reaching higher heights, because the effect occurs only at the detrainment level and so is not felt by shallower clouds.

Arakawa and Schubert (1974) argue that the second process (destabilization tendency) is always weaker than the first process (stabilization). This argument is also consistent with arguments for convective damping put forth by Emanuel *et al.* (1994). However, our preliminary analysis based on Jordan's sounding suggests otherwise: elements of the $\mathcal{K}$ matrix can be positive (*i.e.*, destabilizing) when the precipitation efficiency of the convective cloud is weak. In that case, the cooling by re-evaporation of detrained cloud water is so strong that the given convective plume self-enhances with time. It furthermore promotes the enhancement of convective plumes taller than the type in question.

The second process is akin to the cloud-top entrainment instability hypothesized for the cloud-topped boundary layer (Deadorff 1980, Randall 1980). A major difference is that the process is driven by lateral detrainment rather than by vertical entrainment.

The identified process is likely to explain the recovering process after a dry intrusion, as observed, for example, during the TOGA-COARE period (Parsons *et al.* 2000). Shallow convective clouds are self-enhanced by destabilization of their environment through evaporative cooling of detrained cloud water. The process as a whole contributes to the recovery from dry state to a more normal moist state with the detrainment process contributing to tropospheric moistening.

Once deep convection begins to develop, it tends to stabilize the environmental state, and that contributes to suppression of shallower convective plumes. In this manner, this system described by a $\mathcal{K}$-matrix appears to reproduce a typical life cycle of the tropical convective system associated with the MJO. Benedict and Randall (2007) emphasize the importance of "localized destabilization via low-level warming and moistening" for the MJO.

# 3 Defining the system

## 3.1 System of equations

For a two-mode system the equations for the cloud work function, Eq. 2, read as follows (*cf.*, Yano and Plant 2012b):

$$\begin{aligned} \frac{dA_d}{dt} &= F_d - \gamma_d M_d + \beta_s M_s \\ \frac{dA_s}{dt} &= F_s + \gamma_s M_s - \beta_d M_d \quad . \end{aligned} \tag{3}$$

Here the subscripts $s$ and $d$ label shallow and deep convection, respectively. The $\beta$ and $\gamma$ parameters are elements of the $\mathcal{K}_{ij}$ matrix, discussed in the last section, and defined such that $\gamma_{s,d}$ denotes the effect of the labelled type of convection on the cloud work function for convection of that same type (*i.e.*, the diagonal matrix entries), whereas $\beta_{s,d}$ denotes the effect of the labelled type of convection on the cloud work function for convection of the other type (*i.e.*, the off-diagonal matrix entries). The equations have been written with signs chosen such that $\gamma$ and $\beta$ are expected to be positive from the physical arguments of the last section. Thus, we expect shallow convection to destabilize both shallow and deep convection, and we expect deep convection to stabilize both shallow and deep convection. Note also that the notation for the mass fluxes has been slightly simplified from Eq. 2. Henceforth we use $M$ to denote the cloud–base values. Though Pan and Randall (1998) considered a similar system, they neglected the interactions between the convective modes by setting $\beta_{s,d} = 0$.

The equations for the convective kinetic energy, Eq. 1, read as follows

$$\begin{aligned} \frac{dK_d}{dt} &= M_d A_d - \frac{K_d}{\tau_d} \\ \frac{dK_s}{dt} &= M_s A_s - \frac{K_s}{\tau_s}. \end{aligned} \tag{4}$$

Here we have assumed that the dissipation $D$ for each mode can been characterized in terms of $\tau_{s,d}$, a constant dissipation time scale.

In order to close the energy cycle of the convective system defined by Eqs. 3,4, we also introduce a functional relationship between the convective kinetic energy and the mass flux. This is given by

$$\begin{aligned} K_d &= \alpha_d M_d^p \\ K_s &= \alpha_s M_s^p \end{aligned} \tag{5}$$

with constants $\alpha_d$, $\alpha_s$, and $p$.

In the following, we consider the cases of $p = 2$ and $p = 1$ in order. Pan and Randall (1998) considered the case with $p = 2$, whereas Yano and Plant (2012a) focussed on the case with $p = 1$. Although cloud–resolving model studies as well as statistical theories (Emanuel and Bister 1996, Shutts and Gray 1999, Parodi and Emanuel 2009) clearly favour the case with $p = 1$ as reviewed in Yano and Plant (2011, 2012a), it is fair to say that the evidence is not overwhelming. Note that although the choice $p = 1$ may at first sight be objected to on dimensional grounds, this objection is not in fact substantiated, as discussed in Appendix A.

### 3.2 Estimate of physical parameters

An estimate for the cloud–work function consumption rate $\gamma_d$ was presented by Yano and Plant (2012a). Specifically they argued that

$$\gamma_d \approx \int_{z_b}^{z_t} g \frac{\eta^2}{\rho T_0} \frac{\partial \overline{\theta}}{\partial z} \sim h \frac{g}{\rho_B T_0} \frac{\partial \overline{\theta}}{\partial z} \tag{6}$$

where $z_b$ and $z_t$ are cloud base and cloud top respectively, $\eta$ is the vertical profile of mass flux after normalization by the cloud-base value, $\rho$ is the density, $T_0$ a reference temperature and $\overline{\theta}$ the enviromental potential temperature. The vertical extent of convection is denoted as $h = z_t - z_b$. This expression assumes that the dominant contribution is warming induced by compensating descent, as discussed in Section 2. Yano and Plant (2012a) took the numerical values of $g \sim 10$ ms$^{-2}$, $h \sim 10^4$ m, $\rho \sim 1$ kgm$^{-3}$, $T_0 \sim 300$ K and $\partial\overline{\theta}/\partial z \sim 3 \times 10^{-3}$ Km$^{-1}$ to obtain an order of magnitude estimate of 1 Jm$^2$ kg$^{-2}$. They further state that an explicit evaluation of the integral for an example profile suggested an additional factor of 2. We therefore take $\gamma_d = 2$ Jm$^2$ kg$^{-2}$ here.

The effect of deep convection on the shallow convection work function is assumed to be dominated by the same physical process, and this leads to the estimate

$$\beta_d \approx \int_{z_b}^{z_{t,s}} g \frac{\eta_d \eta_s}{\rho T_0} \frac{\partial \overline{\theta}}{\partial z} \tag{7}$$

The estimate is similar to that in Eq. 6, but there are numerical differences in that $h \sim 10^3$ m is a more suitable value for the vertical extent of shallow convection, and an explicit evaluation now suggests that a factor of $\sim 1$ arises from the normalized integral. Hence, we take $\beta_d = 0.1$ Jm$^2$ kg$^{-2}$.

The effects of shallow convection are described by the parameters $\gamma_s$ and $\beta_s$ and are expected to be dominated by the evaporation of detraining cloud

condensate as argued in Section 2. Relevant expressions for this process are given in Eq. (B37) of Arakawa and Schubert (1974) but in their formulation they are clearly rather sensitive to the value of the entrainment rate, and a detailed cloud model for shallow convection would be required in order to compute these parameters reliably. Some direct evaluations of the $\mathcal{K}_{ij}$ matrix were performed by Yano using a very simple cloud model similar to the entraining plume model of Arakawa and Schubert (1974). These evaluations suggest that $\gamma_s \sim \beta_d$ and $\beta_s \sim \gamma_d$ might be reasonable but it must be recognized that any estimates for $\gamma_s$ and $\beta_s$ are necessarily rather uncertain and possibly the parameters have an important case-to-case dependency. Motivated also by the fact that cases of particular interest arise for $\gamma_s/\beta_s = \beta_d/\gamma_d$ (as will be explained in the analysis below, in Section 4.4 especially), we take $\gamma_s = 0.1$ Jm$^2$ kg$^{-2}$ and $\beta_s = 2$ Jm$^2$ kg$^{-2}$ as being our default parameter choices.

There is little other information available in the literature on typical values for elements of $\mathcal{K}_{ij}$. An exception is a very brief remark on p142 of Randall and Pan (1993) which states that a typical value for $\gamma_s$ is of order 10 times smaller than that for $\gamma_d$. The estimates used here are certainly consistent with that remark.

A typical value for the convective kinetic energy dissipation rate is also not well constrained theoretically (*cf.*, Yano and Plant, 2012a). However recent analysis of cloud–resolving modelling data by Cathy Hohenegger (2011, personal communication) suggests $\tau_s \sim \tau_d \sim 10^3$ s. Note that this estimate is not able to distinguish between shallow and deep convection, unfortunately.

The above parameters are required independently of the choice of $p$. In the next two subsections we discuss estimates of further parameters that are more specific to the cases with $p = 2$ and $p = 1$, respectively.

### 3.2.1 Estimate of physical parameters for the $p = 2$ case

In this case, the proportionality constant $\alpha$ appearing in Eq. 5 (with subscripts $d$ and $s$ to be added as required) is defined by

$$\alpha = \int_{z_b}^{z_t} \frac{\eta^2}{2\rho\sigma_c} dz \tag{8}$$

(Yano and Plant, 2012a). The notation has been already defined with the exception of $\sigma_c$, the fractional convective cloud area.

For the purposes of estimating an order of magnitude, we can write

$$\alpha \sim \frac{h}{\rho\sigma_c} \tag{9}$$

Taking $h$ and $\rho$ as estimated previously and $\sigma_c \sim 10^{-1}$ for both modes, we obtain $\alpha_d \sim 10^5$ m$^4$ kg$^{-1}$ and $\alpha_s \sim 10^4$ m$^4$ kg$^{-1}$.

### 3.2.2 Estimate of physical parameters for the $p = 1$ case

In this case, the proportionality constant $\alpha$ appearing in Eq. 5 is defined by

$$\alpha = w_b \int_{z_b}^{z_t} \frac{\rho_b}{\rho} \frac{\sigma_b}{\sigma_c} \frac{\eta^2}{2} dz \tag{10}$$

(Yano and Plant, 2012a). Here a subscript $b$ has been introduced in order to denote quantites evaluated at cloud base. The $\alpha$ parameter may be estimated as

$$\alpha \sim h w_b \tag{11}$$

again with subscripts $s$ and $d$ to be added appropriately. Taking the same values for $h$ as above, along with $w_b \sim 1$ ms$^{-1}$ for both modes, we obtain $\alpha_d \sim 10^4$ m$^2$ s$^{-1}$ and $\alpha_s \sim 10^3$ m$^2$ s$^{-1}$.

It is worth noting at this point that for the $p = 1$ case, stationary values for the cloud work functions can be determined directly from Eq. 4 using the parameters that have been presented. Denoting these stationary values with a subscript 0, they are

$$\begin{aligned} A_{d0} &= \frac{\alpha_d}{\tau_d} \sim \frac{10^4}{10^3} \sim 10 \text{ Jkg}^{-1} \\ A_{s0} &= \frac{\alpha_s}{\tau_s} \sim \frac{10^3}{10^3} \sim 1 \text{ Jkg}^{-1}. \end{aligned} \tag{12}$$

## 4 Analysis of the system: the $p = 2$ case

Substitution of Eq. 5 with $p = 2$ into Eq. 4 gives

$$\begin{aligned} \dot{M}_s &= \frac{A_s}{2\alpha_s} - \frac{M_s}{2\tau_s} \\ \dot{M}_d &= \frac{A_d}{2\alpha_d} - \frac{M_d}{2\tau_d} \end{aligned} \tag{13}$$

while Eq. 3 is restated here as

$$\begin{aligned} \dot{A}_s &= \gamma_s M_s - \beta_d M_d + F_s \\ \dot{A}_d &= -\gamma_d M_d + \beta_s M_s + F_d \end{aligned} \tag{14}$$

We have introduced a dot in order to denote the time derivative. Eqs. 13 and 14 define the system with $p = 2$ as a set of four linear differential equations with constant coefficients. This is in marked contrast to the case with $p = 1$ to be considered in Section 5, as the latter system is nonlinear. Although we believe that $p = 1$ is more realistic than $p = 2$ (Section 3.1), it is nonetheless of interest to examine the two-mode system with $p = 2$. The linearity greatly facilitates the analysis while leaving the overall behaviour of the coupled system qualitatively simliar. Thus, the analysis of the case with $p = 2$ provides some useful insights also for the case with $p = 1$.

In order to develop a feel for the coupled system, we first consider shallow and deep convection separately in Sections 4.1 and 4.2 respectively. We then turn to a special case of the coupled system in Section 4.3 in order to show some simplified examples of analytical solutions and numerical demonstrations. A more general analysis of the system is then presented in Sections 4.4 and 4.5. We continue in Section 4.6 with perturbation expansions about some limiting cases followed by an analysis of the conditions needed for a periodic solution in Section 4.7 and a summary of the $p = 2$ system in Section 4.8.

### 4.1 Shallow convection only

The equations for the shallow mode only are

$$\begin{aligned} \dot{M}_s = &\quad \frac{A_s}{2\alpha_s} - \frac{M_s}{2\tau_s} \\ \dot{A}_s = &\quad F_s + \gamma_s M_s \end{aligned} \tag{15}$$

and we neglect any large-scale forcing of shallow convection by setting $F_s = 0$.

Cloudy air is detrained from the top of shallow convection and re–evaporates as soon as it is detrained. This induces evaporative cooling, which further destabilizes the atmosphere. The re–evaporative cooling tendency dominates over the effects of diabatic warming by compensative descent for shallow convection, because it is only weakly precipitating. This is expressed by a positive value for $\gamma_s$, so that shallow convection increases the cloud work function, $A_s$. That increase in turn tends to increase the shallow convective mass flux, $M_s$, through the first term on the right hand side of the mass flux evolution equation.

Substituting a solution $M_s = M_s(0)e^{\sigma t}$ and $A_s = A_s(0)e^{\sigma t}$, we obtain

$$\sigma^2 + \frac{\sigma}{2\tau_s} - \frac{\gamma_s}{2\alpha_s} = 0 \tag{16}$$

so that

$$\sigma = -\frac{1}{4\tau_s} \pm \frac{1}{4\tau_s}\left(1 + \frac{8\tau_s}{\tau_{As}}\right)^{1/2} \tag{17}$$

where

$$\tau_{As} = (\alpha_s/\gamma_s)^{1/2} \sim 10^{5/2} \sim 300 \text{ sec} \tag{18}$$

can be interpreted as a characteristic time–scale associated with the shallow cloud work function. Based on the parameter choices of Section 3.2, $\tau_{As} = 10^{5/2} \sim 316$ s.

Owing to the solution from the positive sign of the square root above, the shallow system is exponentially growing with time, regardless of the mass–flux damping time–scale, $\tau_s$. Thus the shallow-only system is self-destabilizing. An example integration is shown in Fig. 1.

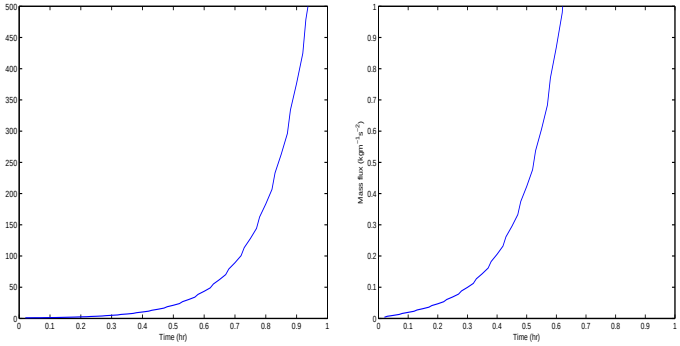


Figure 1: Solution for the unforced shallow mode alone in the $p = 2$ system. The parameters are the default set described in Section 3.2. The initial conditions are $M_s(0) = 10^{-3}$ kgm$^{-2}$s$^{-1}$, $A_s(0) = 1$ Jkg$^{-1}$. On the left and right respectively are shown the time series of the cloud work function and the mass flux.

With the inclusion of forcing it is straightforward to confirm that the eigenvalues are unaltered and the solution is shifted to

$$M_s = M_s(0)e^{\sigma t} - \frac{F_s}{\gamma_s}(1 - e^{\sigma t}) \tag{19}$$

$$A_s = A_s(0)e^{\sigma t} - \frac{\alpha_s F_s}{\gamma_s \tau_s}(1 - e^{\sigma t}) \tag{20}$$

thereby changing the details of the solution but not its basic character.

### 4.2 Deep convection only

The equations for the deep mode only are

$$\begin{aligned} \dot{M}_d = & \quad \frac{A_d}{2\alpha_d} - \frac{M_d}{2\tau_d} \\ \dot{A}_d = & \quad F_d - \gamma_d M_d \end{aligned} \tag{21}$$

again neglecting the large–scale forcing, $F_d = 0$.

Deep convection grows at a rate proportional to the cloud work function. However, the generated deep–convective mass flux consumes the cloud work function, with the notion of convective damping (*cf.*, Emanuel *et al.* 1994).

Neglecting any large-scale forcing of deep convection, $F_d = 0$, and substituting a solution $M_d = M_d(0)e^{\sigma t}$ and $A_d = A_d(0)e^{\sigma t}$ then we obtain

$$\sigma^2 + \frac{\sigma}{2\tau_d} + \frac{\gamma_d}{2\alpha_d} = 0 \tag{22}$$

so that

$$\sigma = -\frac{1}{4\tau_d} \pm \frac{1}{4\tau_d}\left(1 - \frac{8\tau_d}{\tau_{Ad}}\right)^{1/2} \tag{23}$$

where

$$\tau_{Ad} = (\alpha_d/\gamma_d)^{1/2}. \tag{24}$$

Based on the parameter choices of Section 3.2, $\tau_{Ad} = (5 \times 10^4)^{1/2} \sim 223$ s.

Thus, the unforced deep convective system is always damping, regardless of the parameter choices. For $\tau_{Ad} > 8\tau_d$ there are two purely damping modes, whilst for $\tau_{Ad} < 8\tau_d$, the system exhibits a damping oscillations with a period of $8\pi\tau_d(8\tau_d/\tau_{Ad} - 1)^{-1/2}$. An example of a strongly damped oscillation is shown for the default parameters in Fig. 2.

### 4.3 A special case: Mass flux equilibrates more quickly than work function

Henceforth we consider the full system in which shallow and deep convection are coupled. In the following Section 4.4, we consider the general case for any parameter set. Before doing so, it will be instructive to consider a particular limit which provides some insight into how the coupled system can behave. Specifically, the present subsection considers a regime in which the mass flux evolution equations, Eq. 13, come into an equilibrium much more quickly than the cloud work function equations, Eq. 14. Such a situation arises

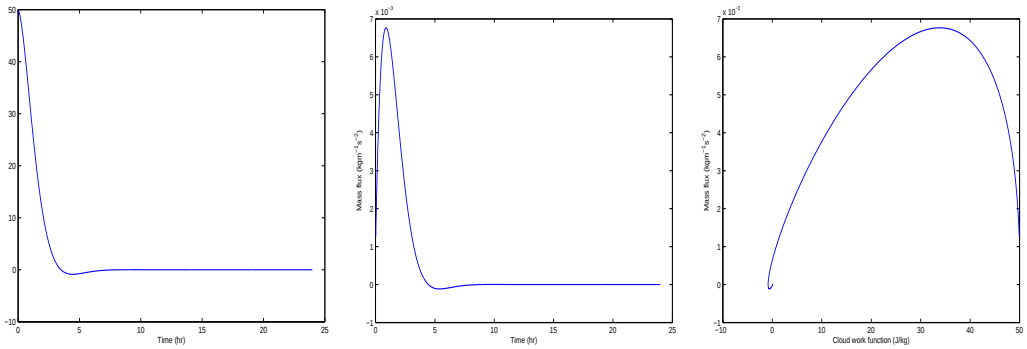


Figure 2: Solution for the unforced deep mode alone in the $p = 2$ system. The parameters are the default set described in Section 3.2. The initial conditions are $M_d(0) = 10^{-3}$ kgm$^{-2}$s$^{-1}$, $A_d(0) = 50$ Jkg$^{-1}$. From left to right are shown: the time series of the cloud work function, the time series of mass flux, and the trajectory in the phase space of the cloud work function (horizontal axis) and mass flux (vertical axis).

when the kinetic energy dissipation time scales are much shorter than the cloud–work function time scales: *i.e.*, if

$$\tau_s \sim \tau_d \ll \tau_{As} \sim \tau_{Ad}. \tag{25}$$

Taking the estimates from Sections 4.1 and 4.2, $\tau_{Ad} \sim \tau_{As} \sim 300$ s, which is comparable with the default dissipation time scales $\tau_s = \tau_d = 10^3$s. Thus the limit is unlikely to be a good approximation for most situations of physical interest, but it is nonetheless convenient for conceptual consideration.

Under this limit, Eq. 13 provides an approximate functional relationship between the cloud work functions and the mass fluxes,

$$\begin{aligned} A_s &\approx \frac{\alpha_s}{\tau_s} M_s \\ A_d &\approx \frac{\alpha_d}{\tau_d} M_d. \end{aligned} \tag{26}$$

Substitution of these relationships into Eq. 14 yields the relatively slow evolution of the unforced cloud work functions as:

$$\begin{aligned} \dot{A}_s &= \hat{\gamma}_s A_s - \hat{\beta}_d A_d \\ \dot{A}_d &= -\hat{\gamma}_d A_d + \hat{\beta}_s A_s \end{aligned} \tag{27}$$

where we have introduced the notation

$$\hat{\gamma}_s = \frac{\gamma_s \tau_s}{\alpha_s}, \qquad \hat{\beta}_s = \frac{\beta_s \tau_s}{\alpha_s},$$
$$\hat{\gamma}_d = \frac{\gamma_d \tau_d}{\alpha_d}, \qquad \hat{\beta}_d = \frac{\beta_d \tau_d}{\alpha_d}. \tag{28}$$

Note that $\hat{\gamma}_s = \tau_s/\tau_{As}^2$ and $\hat{\gamma}_d = \tau_d/\tau_{Ad}^2$ are the slow rates at which the cloud work functions evolve.

Considering a solution of the form $\sim e^{\sigma t}$ results in the eigenfrequency equation

$$\sigma^2 + (\hat{\gamma}_d - \hat{\gamma}_s)\sigma - \hat{\gamma}_s\hat{\gamma}_d + \hat{\beta}_s\hat{\beta}_d = 0 \tag{29}$$

with solution

$$\sigma = \frac{1}{2}\left\{\hat{\gamma}_s - \hat{\gamma}_d \pm \left[(\hat{\gamma}_s - \hat{\gamma}_d)^2 - 4(\hat{\beta}_s\hat{\beta}_d - \hat{\gamma}_s\hat{\gamma}_d)\right]^{1/2}\right\} \tag{30}$$

Thus, we can have three types of solution:

(i) If $\hat{\gamma}_s > \hat{\gamma}_d$ then the solution grows (possibly a growing oscillation or possibly pure exponential growth);

(ii) If $\hat{\gamma}_s = \hat{\gamma}_d$ then the solution will be neutral if $\hat{\beta}_s\hat{\beta}_d = \hat{\gamma}_s\hat{\gamma}_d$, growing if $\hat{\beta}_s\hat{\beta}_d < \hat{\gamma}_s\hat{\gamma}_d$, or purely oscillatory if $\hat{\beta}_s\hat{\beta}_d > \hat{\gamma}_s\hat{\gamma}_d$;

(iii) if $\hat{\gamma}_s < \hat{\gamma}_d$ then the solution is damping with an oscillation if the argument of the square root is negative, pure damping if the argument of the square root is positive and if $\hat{\beta}_s\hat{\beta}_d > \hat{\gamma}_s\hat{\gamma}_d$, and growing if the argument of the square root is positive and if $\hat{\beta}_s\hat{\beta}_d < \hat{\gamma}_s\hat{\gamma}_d$.

Figs. 3, 4 and 5 give examples respectively of numerical solutions for a growing set of parameters with case (i), an oscillatory set of parameters with case (ii) and a damping set of parameters with case (iii). As noted above, the limiting case considered in this subsection is primarily of conceptual interest to demonstrate the behaviour. To produce these figures we chose parameter values considerably removed from the default set of Section 3.2 in order to respect the limiting approximation. A consequence of the choices is that the cloud work functions and mass fluxes sometimes take negative values during the resulting evolution. Note also that each example exhibits a rapidly decaying transient for the mass flux over the first 2 hr before the longer time behaviour becomes apparent.

In physical terms, these limiting analytical results show that the system may be growing or damping depending on whether self–growing shallow

convection ($\hat{\gamma}_s$) or self–damping deep convection ($\hat{\gamma}_d$) dominates respectively. However, if the destabilization and stabilization tendencies can be balanced then we can obtain a neutral state.

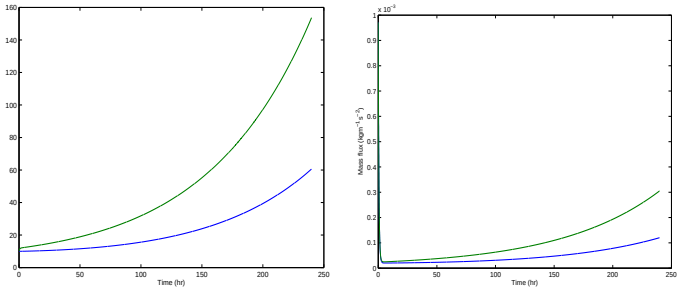


Figure 3: Solution for the unforced $p = 2$ system with parameters chosen to illustrate case (i) of Section 4.3. Blue is for the deep mode and green for the shallow mode. The parameters are $\gamma_d = 1, \gamma_s = 2, \beta_d = \beta_s = 1$ Jm$^2$ kg$^{-2}$, $\alpha_d = \alpha_s = 5 \times 10^8$ m$^4$ kg$^{-1}$ and $\tau_d = \tau_s = 10^3$ s. Note that these give values of $\tau_{As} = 1.6 \times 10^5$ s and $\tau_{Ad} = 2.2 \times 10^5$ s. The initial conditions are $M_d(0) = M_s(0) = 10^{-3}$ kgm$^{-2}$s$^{-1}$ and $A_d(0) = A_s(0) = 10$ Jkg$^{-1}$. Shown in the same format as in Fig. 1.

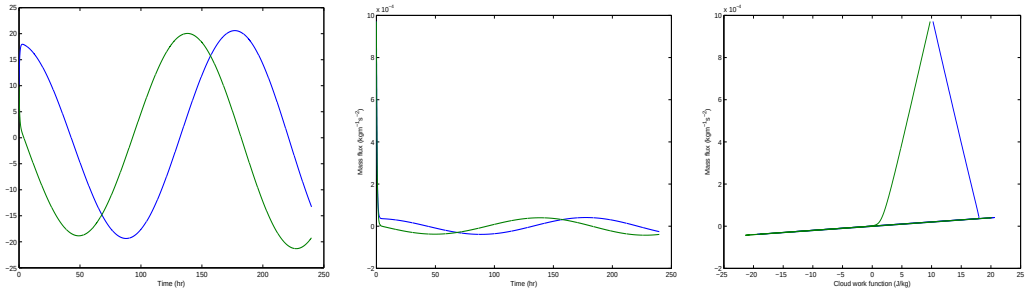


Figure 4: Solution for the unforced $p = 2$ system with parameters chosen to illustrate case (ii) of Section 4.3. Blue is for the deep mode and green for the shallow mode. The parameters are $\gamma_d = \gamma_s = 1, \beta_d = \beta_s = 5$ Jm$^2$ kg$^{-2}$, $\alpha_d = \alpha_s = 5 \times 10^8$ m$^4$ kg$^{-1}$ and $\tau_d = \tau_s = 10^3$ s. Note that these give values of $\tau_{As} = \tau_{Ad} = 2.2 \times 10^5$ s. The initial conditions are $M_d(0) = M_s(0) = 10^{-3}$ kgm$^{-2}$s$^{-1}$ and $A_d(0) = A_s(0) = 10$ Jkg$^{-1}$. Shown in the same format as in Fig. 2.

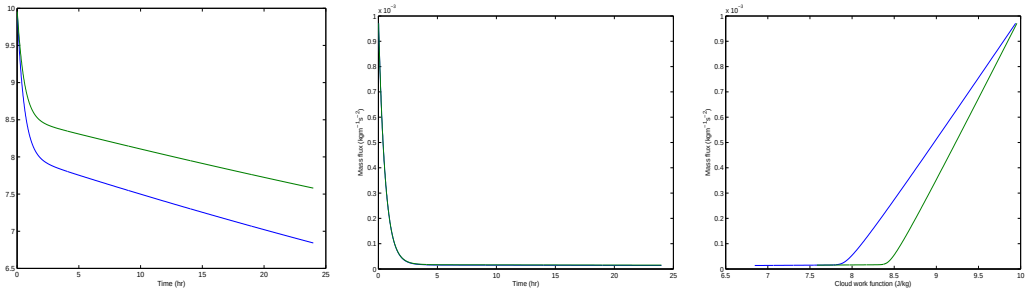


Figure 5: Solution for the unforced $p = 2$ system with parameters chosen to illustrate case (iii) of Section 4.3. Blue is for the deep mode and green for the shallow mode. The parameters are $\gamma_d = 2, \gamma_s = 0.25, \beta_d = \beta_s = 1$ Jm$^2$ kg$^{-2}$, $\alpha_d = \alpha_s = 5 \times 10^8$ m$^4$ kg$^{-1}$ and $\tau_d = \tau_s = 10^3$ s. Note that these give values of $\tau_{As} = 1.6 \times 10^5$ s and $\tau_{Ad} = 4.5 \times 10^5$ s. The initial conditions are $M_d(0) = M_s(0) = 10^{-3}$ kgm$^{-2}$s$^{-1}$ and $A_d(0) = A_s(0) = 10$ Jkg$^{-1}$. Shown in the same format as in Fig. 2.

### 4.4 General case

We now proceed to consider the *general* case of the coupled $p = 2$ system, Eqs. 13 and 14, without approximation.

As a linear system of ordinary differential equations with constant coefficients it has a solution of the form $e^{\sigma t}$ for each of the dependent variables, and a quartic equation for $\sigma$ is easily derived. However, the obtained equation for the eigenfrequency is not physically illuminating and not stated here.

The discussion of the special case in Section 4.3 reveals that the overall behaviour of the unforced coupled system is determined by a competition between the growing tendency of shallow convection and the damping tendency of deep convection. For most parameter choices, one of those tendencies is dominant and convection either dies out or explodes. However, there may be parameter settings that allow a balance to be realized between these two tendencies (*e.g.*, Fig. 4). A natural question to ask is under what conditions can we obtain such a balanced solution. It turns out that many of the same considerations arise for the nonlinear coupled system with $p = 1$ (Section 5.3).

### 4.4.1 The vanishing determinant

Consider the cloud work function tendency equations, Eq. 14, and look for a solution which is non-trivial in the absence of forcing. By non-trivial we mean a solution in which both $M_s$ and $M_d$ neither tend to zero nor tend to infinity, even for very long times. This is clearly a strong constraint on the problem. It is not physically reasonable to imagine that all of the parameters of the coupled system stay fixed in perpetuity, and so in practice we may be interested in cases where the coupled system does decay or grow, so long as that occurs very slowly. Nonetheless we will pursue this strict constraint, while bearing in mind that it is likely to lead us to overly restrictive constraints on the parameters.

A non-trivial solution in the above sense can be achieved if the solution becomes periodic so that $A_s$ and $A_d$ vary over time but they do so in such a way that their time-averaged variation vanishes over some finite period $T$.

Setting the forcing to zero in Eq. 14 and denoting by an overbar the time average over period $T$ then the solutions of interest occur for

$$\begin{aligned} -\gamma_d \overline{M_d} + \beta_s \overline{M_s} &= 0 \\ \gamma_s \overline{M_s} - \beta_d \overline{M_d} &= 0 \end{aligned} \tag{31}$$

so that

$$\beta_d \beta_s = \gamma_d \gamma_s. \tag{32}$$

In other words, the determinant of the $\mathcal{K}_{ij}$ matrix must vanish for a non-trivial solution in the absence of forcing. For the remainder of Section 4 we will assume that this condition is indeed satisfied and examine the consequences.

There are several important remarks that should be made about this condition. First, note that the argument is easily extended to any number of convective modes. Second, note that the argument depends on the cloud work function tendency equations only. As such, the condition is entirely independent of the assumed functional form of the kinetic energy dissipation in Eq. 4 and of the assumed functional relationship between convective kinetic energy and cloud base mass flux. In particular, it is independent of the choice of $p$. Third, we note that the set of default parameter choices discussed in Section 3.2 satisfies the condition. As alluded to earlier, this last point is not accidental, but it nonetheless does illustrate that the condition may be satisfied for physically–plausible parameter settings.

### 4.4.2 Linking the cloud work functions

We are now in a position to simplify the cloud work function tendency equations, Eq. 14. Expressing the unforced equation for shallow convection as

$$\dot{A}_s = \frac{\gamma_s}{\beta_s}\left(\beta_s M_s - \frac{\beta_d \beta_s}{\gamma_s} M_d\right) \tag{33}$$

and using Eq. 32 for the vanishing determinant, we have

$$\dot{A}_s = \frac{\gamma_s}{\beta_s}\left(\beta_s M_s - \gamma_d M_d\right). \tag{34}$$

Next we substitute for the term in brackets on the right-hand-side by using the tendency equation for the evolution of the deep cloud work function. This produces

$$\dot{A}_s = \frac{\gamma_s}{\beta_s}\dot{A}_d \tag{35}$$

Hence (in the absence of forcing) the cloud work function tendencies are proportional for shallow and deep convection.

We can integrate the above equation directly to relate the two work functions as

$$A_s - A_s(0) = \frac{\gamma_s}{\beta_s}\left(A_d - A_d(0)\right). \tag{36}$$

The relationship is a direct consequence of the vanishing determinant and so applies with all the generality discussed in the previous subsection.

As a short aside on the forcing, note that if forcing were to be retained then the two work functions would be related by

$$A_s - A_s(0) = \frac{\gamma_s}{\beta_s}\left(A_d - A_d(0)\right) + \left(F_s - \frac{\gamma_s}{\beta_s}F_d\right)t \tag{37}$$

The term proportional to $t$ prevents a closed orbit solution to the coupled system. However, that term would vanish if

$$F_s = \frac{\gamma_s}{\beta_s}F_d \tag{38}$$

Clearly this includes the case of zero forcing, but it is also interesting to note that forcing could be incorporated into all of the following analysis, provided that it were to be related as above for the two types of convection.

### 4.5 The $p = 2$ equations with vanishing determinant: General considerations

Here we consider the unforced $p = 2$ system with a vanishing determinant but with no other constraints or approximations. Using Eq. 36 just derived above we can eliminate $A_s$ in the prognostic equation for $M_s$ to yield:

$$\dot{M}_s = \frac{A_s(0)}{2\alpha_s} - \frac{\gamma_s A_d(0)}{2\alpha_s\beta_s} + \frac{\gamma_s}{2\alpha_s\beta_s}A_d - \frac{M_s}{\tau_s} \tag{39}$$

We consider the above equation alongside those for the deep mode which are restated here for convenience

$$\dot{M}_d = \frac{A_d}{2\alpha_d} - \frac{M_d}{2\tau_d} \tag{40}$$

$$\dot{A}_d = F_d - \gamma_d M_d + \beta_s M_s \tag{41}$$

We try a solution of the following form

$$\begin{aligned} A_d &= a_0 + a_1 e^{\sigma t} \\ M_d &= d_0 + d_1 e^{\sigma t} \\ M_s &= s_0 + s_1 e^{\sigma t} \quad , \end{aligned} \tag{42}$$

where the coefficients $a_1$, $d_1$ and $s_1$ can be expressed in terms of $a_0$, $d_0$ and $s_0$ and the initial conditions,

$$\begin{aligned} a_1 &= A_d(0) - a_0 \\ d_1 &= M_d(0) - d_0 \\ s_1 &= M_s(0) - s_0 \end{aligned} \tag{43}$$

and where the coefficients $a_0$, $d_0$ and $s_0$ can be obtained by substituting in the trial solution and then comparing the constant terms to give

$$\tau_d a_0 = \alpha_d d_0 \tag{44}$$

$$\beta_s s_0 = \gamma_d d_0 \tag{45}$$

$$\frac{s_0}{\tau_s} = \frac{\gamma_s}{\alpha_s\beta_s}d_0 + \frac{A_s(0)}{\alpha_s} - \frac{\gamma_s A_d(0)}{\alpha_s\beta_s} \tag{46}$$

The solution for $a_0$ is easily obtained

$$a_0 = [\beta_s A_s(0) - \gamma_s A_d(0)] \left[\frac{\alpha_s\gamma_d\tau_d}{\alpha_d\tau_s} - \gamma_s\right]^{-1} \tag{47}$$

whilst $s_0$ and $d_0$ are simply proportional to this, as given in Eqs. 44 and 45.

Comparing coefficients of the exponential terms that occur in the trial solution gives three equations in terms of $a_1$, $d_1$, $s_1$ and $\sigma$. This reduces to the eigenequation

$$\sigma^3 + \frac{\sigma^2}{2}\left(\frac{1}{\tau_d} + \frac{1}{\tau_s}\right) + \frac{\sigma}{4}\left[\frac{1}{\tau_d\tau_s} + 2\left(\frac{\hat{\gamma}_d}{\tau_d} - \frac{\hat{\gamma}_s}{\tau_s}\right)\right] + \frac{1}{4\tau_d\tau_s}(\hat{\gamma}_d - \hat{\gamma}_s) = 0 \quad (48)$$

which we have rewritten in terms of the rescaled (self–)interaction coefficients introduced in Eq. 28. Note that in terms of these rescaled coefficients the vanishing determinant condition reads

$$\hat{\beta}_d\hat{\beta}_s = \hat{\gamma}_d\hat{\gamma}_s. \quad (49)$$

An explicit formal solution can be written for the above eigenequation, but is not very illuminating. Nonetheless, we can offer some useful remarks. A cubic equation may have three real roots, or else one real root with one complex–conjugate pair. In order for the solution not to explode, we require that any real roots are negative or zero, whereas any complex conjugate roots have a negative real part. In either case, the product of the three roots must be negative or zero[2]. Since the product of the roots is given by minus the constant term in Eq. 48 it follows that to avoid an exploding solution

$$\hat{\gamma}_d \geq \hat{\gamma}_s \quad (50)$$

Physically this requirement is for the damping rate of the deep cloud work function, $\hat{\gamma}_d$, to exceed the generation rate of the shallow cloud work function, $\hat{\gamma}_s$.

A non-exploding case with three negative real roots will decay towards an equilibrium state with $A_d = a_0$, $M_d = d_0$, $M_s = s_0$, whilst a case with complex roots may be more interesting as pure imaginary roots will decay towards a purely oscillating solution. It is possible to write down an explicit inequality in order for a cubic equation to have non-real roots, but again that is not physically illuminating and we cannot say from that whether those roots are explosive.

Finally, we close this subsection by remarking that the eigenequation 48 does not include $\hat{\beta}_s$ or $\hat{\beta}_d$. Thus, provided that these interaction coefficients are such as to produce a vanishing determiant their value does not otherwise affect the character of the solution.

[2]Moreover, the sum of roots must be negative. This is guaranteed since the coefficient of the quadratic term in Eq. 48 is positive definite.

## 4.6 The $p = 2$ equations with vanishing determinant: Perturbation approaches

In the previous subsection, we derived the cubic eigenequation 48 for the general case of the unforced $p = 2$ system with vanishing determinant. However, we noted that a formal solution to this equation is not physically instructive. Therefore, in the following subsections we specialize to situations where $\tau_s \approx \tau_d$ (Sections 4.6.1 and 4.6.2), where $\tau_s \ll \tau_d$ (Section 4.6.3) and where $\tau_s \gg \tau_d$ (Section 4.6.4), in order to illustrate the behaviour of the system in a more useful way. First we consider the case of $\tau_s = \tau_d$ in Section 4.6.1, and then in Section 4.6.2 we consider small departures from equality of the dissipation time scales, by means of a perturbation expansion.

The starting point for these analyses is to express the eigenequation in terms of the new variables

$$\begin{aligned} \xi_s &= \sigma(2\sigma\tau_s + 1) \\ \xi_d &= \sigma(2\sigma\tau_d + 1) \end{aligned} \tag{51}$$

in terms of which it reads

$$\xi_s\xi_d + \hat{\gamma}_d\xi_s - \hat{\gamma}_s\xi_d + (\hat{\beta}_s\hat{\beta}_d - \hat{\gamma}_s\hat{\gamma}_d) = 0 \tag{52}$$

This is the full quartic equation, which can easily be seen to reduce a cubic equation if the term in brackets vanishes, as occurs for the vanishing determinant condition of Eq. 49.

### 4.6.1 The case of $\tau_s = \tau_d$

Assuming a vanishing determinant, and specializing also to the case of $\tau_s = \tau_d$ then we can work in terms of the variable $\xi = \xi_s = \xi_d = \sigma(2\sigma\tau + 1)$ where $\tau = \tau_s = \tau_d$. This variable satisfies the equation

$$\xi^2 + (\hat{\gamma}_d - \hat{\gamma}_s)\xi = 0 \tag{53}$$

leading to

$$\xi = 0 \quad \text{or} \quad \xi = \hat{\gamma}_s - \hat{\gamma}_d. \tag{54}$$

By solving the definition of $\xi$ to obtain $\sigma$, we find that

$$\sigma = -\frac{1}{4\tau} \pm \left[\left(\frac{1}{4\tau}\right)^2 + \frac{\xi}{2\tau}\right]^{1/2} \tag{55}$$

so that the eigenfrequencies are:

$$\sigma = -\frac{1}{2\tau} \tag{56}$$

$$\sigma = -\frac{1}{4\tau} \pm \left[ \left( \frac{1}{4\tau} \right)^2 + \frac{1}{2\tau} (\hat{\gamma}_s - \hat{\gamma}_d) \right]^{1/2} \tag{57}$$

Thus the characteristics of the system are determined by $\hat{\gamma}_s - \hat{\gamma}_d$. If $\hat{\gamma}_d < \hat{\gamma}_s$ and shallow convection dominates then then there is a growing solution without oscillation (the square root term produces a positive eigenfrequency when the square root is taken with a plus). If $\hat{\gamma}_s + 1/(8\tau) > \hat{\gamma}_d > \hat{\gamma}_s$ then deep convection is weakly dominant and there is a damping solution (the square root term is real but is not large enough in magnitude to be able to change the sign of $\sigma$). If $\hat{\gamma}_d > \hat{\gamma}_s + 1/(8\tau)$ then deep convection is more strongly dominant and there is a damping solution with an oscillation (the square root is imaginary).

We can of course solve the cubic eigenequation 48 numerically. Fig. 6 shows the phase diagram produced, which is easily checked to be consistent with the analysis just presented.

It should be noticed that do not find any possibility for a purely imaginary (i.e., perpetually and stably periodic) solution. This is because any solution with an imaginary eigenvalue also has a negative real part for that eigenvalue. Or, in other words, because the interface between positive and negative real eigenvalues occurs where there is no imaginary part to the eigenvalue. There is no point of contact between regions I and III in the phase diagram.

To illustrate some particular cases taken from Fig. 6, Figs. 7, 8 and 9 give examples respectively of numerical solutions in regions: (I) a growing solution; (II) pure decay to constant values; and, (III) decay–with–oscillation.

### 4.6.2 With a slight deviation from $\tau_s = \tau_d$

We now consider the $p = 2$ system with vanishing determinant for unequal $\tau$ but with the shallow and deep time scales being close together. The main question is whether a distinction between the time scales is able to alter the phase diagram in such a way as to be able to produce a periodic solution.

We introduce the notation

$$\Delta\xi \equiv (\xi_s - \xi_d)/2 \tag{58}$$

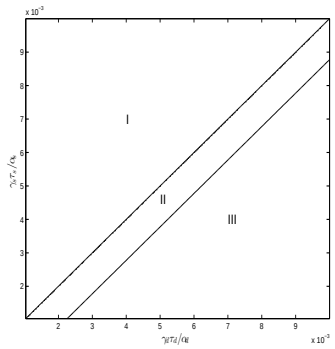


Figure 6: Numerically–generated phase diagram for the $p = 2$ system with vanishing determinant. The default parameters described in Section 3.2 are used for $\alpha_s$ and $\alpha_d$, while a parameter choice for $\beta_s$ and $\beta_d$ is not required. The values for $\gamma_s$ and $\gamma_d$ have been varied to produce the diagram. The parameters $\tau_s$ and $\tau_d$ have been set to $10^2$ s here rather than their default values of $10^3$ s, in order to clarify the presence of region II, which is much thinner with the default values. Region I produces exploding cases ($\gamma_s > \gamma_d$), region II has pure decay cases ($\hat{\gamma}_s + 1/(8\tau) > \hat{\gamma}_d > \hat{\gamma}_s$) and region III has decay–with–oscillation cases ($\hat{\gamma}_d > \hat{\gamma}_s + 1/(8\tau)$). The regions are separated by plotting two contours for the eigenvalue with the largest real part. The contour where that real part is zero separates regions I and II. The contour where the imaginary part of that same eigenvalue is zero separates regions II and III.

with

$$\begin{aligned} \xi_d &= \xi - \Delta\xi \\ \xi_s &= \xi + \Delta\xi \end{aligned} \tag{59}$$

We furthermore introduce

$$\begin{aligned} \tau_0 &\equiv (\tau_s + \tau_d)/2 \\ \Delta\tau &\equiv \tau_s - \tau_d \end{aligned} \tag{60}$$

so that the relation

$$\Delta\xi = \sigma^2(\tau_s - \tau_d) = \sigma^2\Delta\tau. \tag{61}$$

follows immediately from the definition of terms. The assumption that the two convective time scales are close together means that we can take $\xi \gg |\Delta\xi|$ or $\tau \gg |\Delta\tau|$ below.

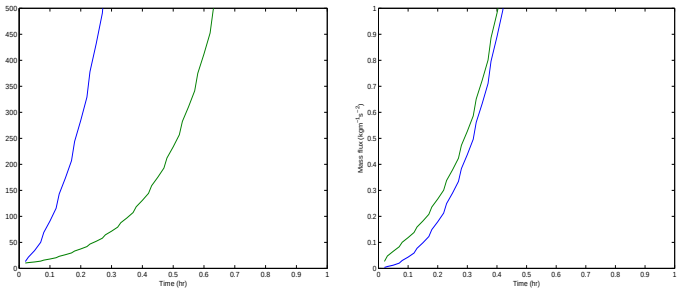

Figure 7: Solution for the unforced $p = 2$ system with parameters chosen to illustrate region I of Fig. 6. Blue is for the deep mode and green for the shallow mode. The parameters are $\gamma_d = 2, \gamma_s = 0.4, \beta_d = 0.2, \beta_s = 4$ Jm$^2$ kg$^{-2}$ and $\tau_d = \tau_s = 10^2$ s, together with the default choices for $\alpha_s$ and $\alpha_d$ described in Section 3.2. Note that these choices give $\hat{\gamma}_s = 4 \times 10^{-3}$ s$^{-1}$ and $\hat{\gamma}_d = 2 \times 10^{-3}$ s$^{-1}$, so that $\hat{\gamma}_s > \hat{\gamma}_d$. The initial conditions are $M_d(0) = M_s(0) = 10^{-3}$ kgm$^{-2}$s$^{-1}$ and $A_d(0) = A_s(0) = 10$ Jkg$^{-1}$. Shown in the same format as in Fig. 1.

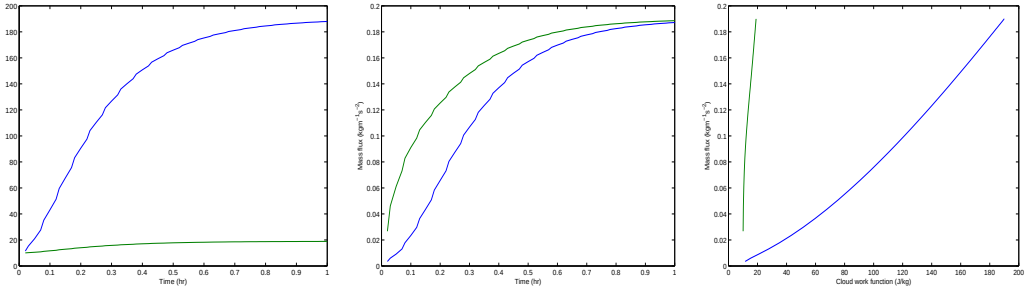

Figure 8: Solution for the unforced $p = 2$ system with parameters chosen to illustrate region II of Fig. 6. Blue is for the deep mode and green for the shallow mode. The parameters are $\tau_d = \tau_s = 10^2$ s, together with the default choices for $\alpha, \beta$ and $\gamma$ described in Section 3.2. Note that these choices give $\hat{\gamma}_s = 10^{-3}$ s$^{-1}$ and $\hat{\gamma}_d = 2 \times 10^{-3}$ s$^{-1}$, so that $\hat{\gamma}_s + 1/8\tau_s > \hat{\gamma}_d > \hat{\gamma}_s$. The initial conditions are $M_d(0) = M_s(0) = 10^{-3}$ kgm$^{-2}$s$^{-1}$ and $A_d(0) = A_s(0) = 10$ Jkg$^{-1}$. Shown in the same format as in Fig. 2.

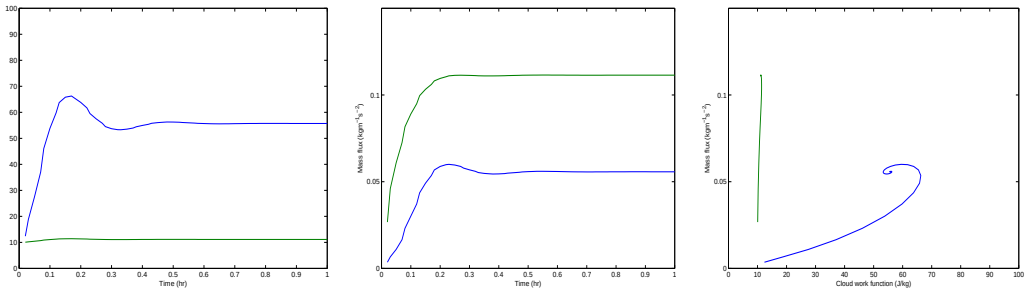

Figure 9: Solution for the unforced $p = 2$ system with parameters chosen to illustrate region III of Fig. 6. Blue is for the deep mode and green for the shallow mode. The parameters are $\gamma_d = 8, \gamma_s = 0.1, \beta_d = 0.2, \beta_s = 4$ Jm$^2$ kg$^{-2}$ and $\tau_d = \tau_s = 10^2$ s, together with the default choices for $\alpha_s$ and $\alpha_d$ described in Section 3.2. Note that these choices give $\hat{\gamma}_s = 10^{-3}$ s$^{-1}$ and $\hat{\gamma}_d = 8 \times 10^{-3}$ s$^{-1}$, so that $\hat{\gamma}_d > \hat{\gamma}_s + 1/8\tau_s$. The initial conditions are $M_d(0) = M_s(0) = 10^{-3}$ kgm$^{-2}$s$^{-1}$ and $A_d(0) = A_s(0) = 10$ Jkg$^{-1}$. Shown in the same format as in Fig. 2.

The eigenfrequency equation for any values of $\tau$ was stated as 52 above. In the limit of equal shallow and deep time scales it reduces to Eq. 53 giving us the leading–order solution $\xi \equiv \xi_0 = 0$ or $\hat{\gamma}_s - \hat{\gamma}_d$ just as in Eq. 54, with corresponding eigenfrequencies as given in Eq. 55. With the notation of the current subsection, these read

$$\sigma_0 = -\frac{1}{4\tau_0} \pm \left[ \left( \frac{1}{4\tau_0} \right)^2 + \frac{\xi_0}{2\tau_0} \right]^{1/2} \tag{62}$$

To obtain the leading corrections to these results for a difference in time scales, we write $\xi = \xi_0 + \xi_1$ and expand the eigenfrequency equation 52 to include first order terms in $\Delta\xi$ and $\xi_1$. We first note that

$$\xi_s \xi_d = (\xi_0 + \xi_1 + \Delta\xi)(\xi_0 + \xi_1 - \Delta\xi) = (\xi_0 + \xi_1)^2 - \Delta\xi^2 \simeq \xi_0^2 + 2\xi_1\xi_0 \tag{63}$$

so that $\Delta\xi$ does not enter into this expression at the leading order. As a result, at first order Eq. 52 is

$$2\xi_0\xi_1 + (\hat{\gamma}_d + \hat{\gamma}_s)\Delta\xi + (\hat{\gamma}_d - \hat{\gamma}_s)\xi_1 = 0 \tag{64}$$

or

$$(2\xi_0 + \hat{\gamma}_d - \hat{\gamma}_s)\xi_1 + (\hat{\gamma}_d + \hat{\gamma}_s)\Delta\xi = 0 \tag{65}$$

leading to

$$\xi_1 = -(2\xi_0 + \hat{\gamma}_d - \hat{\gamma}_s)^{-1}(\hat{\gamma}_d + \hat{\gamma}_s)\Delta\xi \tag{66}$$

For the case of $\xi_0 = 0$ we have $\sigma_0 = 0$ or $\sigma_0 = -1/(2\tau_0)$. The first of these possibilities gives $\Delta\xi = 0$ at leading order and so $\xi_1 = 0$. The second possibility gives

$$\xi_1 = -\left(\frac{\hat{\gamma}_d + \hat{\gamma}_s}{\hat{\gamma}_d - \hat{\gamma}_s}\right)\frac{\tau_s - \tau_d}{4\tau_0^2} = -\lambda_1\Delta\xi \tag{67}$$

where we have defined

$$\lambda_1 \equiv \frac{\hat{\gamma}_d + \hat{\gamma}_s}{\hat{\gamma}_d - \hat{\gamma}_s} \tag{68}$$

For the case of $\xi_0 = \hat{\gamma}_s - \hat{\gamma}_d$ we have

$$\xi_1 = \lambda_1\Delta\xi \tag{69}$$

Expressions 67 and 69 are the first order expressions for the corrections to each of the solutions to $\xi$. However, we wish to translate these corrections into the corresponding corrections to the eigenfrequnecies $\sigma$. In order to make this translation we write $\sigma = \sigma_0 + \sigma_1$, substitute this form into the definition for either of $\xi_s$ or $\xi_d$ (Eq. 51) and expand all variables to first order in the time scale difference. The result is that

$$\sigma_1 = \frac{\xi_1}{4\sigma_0\tau_0 + 1} \tag{70}$$

So for the non-trivial case with $\xi_0 = 0$ we have

$$\sigma_0 = -\frac{1}{2\tau_0} \qquad \sigma_1 = -\xi_1 = \lambda_1\Delta\xi \tag{71}$$

so that

$$\sigma = -\frac{1}{2\tau_0} + \left(\frac{\hat{\gamma}_d + \hat{\gamma}_s}{\hat{\gamma}_d - \hat{\gamma}_s}\right)\frac{\tau_s - \tau_d}{4\tau_0^2} + \mathcal{O}(\tau_s - \tau_d)^2 \tag{72}$$

which is a real correction to a real eigenvalue.

For the case of $\xi_0 = \hat{\gamma}_s - \hat{\gamma}_d$ we have

$$\sigma_0 = -\frac{1}{4\tau_0} \pm \lambda_0 \qquad \sigma_1 = \pm\frac{\lambda_1}{\lambda_0}\frac{\Delta\xi}{4\tau_0} = \pm\frac{\lambda_1}{\lambda_0}\sigma_0^2\frac{\Delta\tau}{4\tau_0} \tag{73}$$

where

$$\lambda_0 = \frac{1}{4\tau_0}\left[1 + 8\tau_0(\hat{\gamma}_s - \hat{\gamma}_d)\right]^{1/2} \tag{74}$$

By further using the relation

$$\sigma_0^2 = \frac{1}{(4\tau_0)^2} + \lambda_0^2 \mp \frac{\lambda_0}{2\tau_0} \tag{75}$$

we obtain the following expression for the correction term

$$\sigma_1 = \pm \frac{\lambda_1}{\lambda_0} \frac{(\tau_s - \tau_d)}{4\tau_0} \left[ \frac{1}{(4\tau_0)^2} + \lambda_0^2 \mp \frac{\lambda_0}{2\tau_0} \right] \tag{76}$$

In summary we obtain

$$\sigma = -\frac{1}{4\tau_0} \pm \lambda_0 \left\{ 1 + \lambda_1 \frac{(\tau_s - \tau_d)}{4\tau_0} \left[ 1 + \frac{1}{(4\tau_0\lambda_0)^2} \mp \frac{1}{2\tau_0\lambda_0} \right] \right\} \tag{77}$$

Since $\lambda_1$ is real, the eigenvalue as a whole must be real unless $\lambda_0$ is imaginary. Simple inspection of Eq. 74 shows that this requires $\hat{\gamma}_d > \hat{\gamma}_s + (1/8\tau_0)$ as was already derived for the case of equal time scales in the previous subsection. Assuming that $\lambda_0$ is indeed imaginary, the next question to ask is whether there are circumstances in which the real part of the eigenvalue vanishes. If so then a periodic solution can be obtained.

The real part of the eigenvalue in this case is

$$-\frac{1}{4\tau_0} - \lambda_0 \left\{ \lambda_1 \frac{(\tau_s - \tau_d)}{4\tau_0} \frac{1}{2\tau_0\lambda_0} \right\} = -\frac{1}{4\tau_0} \left[ 1 + \lambda_1 (\tau_s - \tau_d) \frac{1}{2\tau_0} \right] \tag{78}$$

which will vanish if

$$\tau_d - \tau_s = \frac{2\tau_0}{\lambda_1} = 2\tau_0 \left( \frac{\hat{\gamma}_d + \hat{\gamma}_s}{\hat{\gamma}_d - \hat{\gamma}_s} \right) \tag{79}$$

Given that $\hat{\gamma}_d$ and $\hat{\gamma}_s$ are positive, the factor in brackets in the above equation can have a modulus that is no larger than 1. Thus, in order for the real part to vanish the difference between the shallow and deep time scales must be larger than the mean time scale. Since this contradicts our original assumption that the time scale difference can be treated as a perturbation, the conclusion must be that a periodic solution cannot be obtained for a small time scale difference.

We have checked this analysis numerically by solving the full eigenvalue equation for cases where $\tau_s$ is 10% larger than $\tau_d$ and vice versa. The resulting phase diagrams are shown in Fig. 10 and may be compared with Fig. 6. The lines separating regions I/II and II/III have different slopes for $\tau_s \neq \tau_d$ and so tend towards each other in a part of phase space. Thus, the analysis in this section does raise the possibility that the system can produce a periodic solution, but demonstrates that this will not occur in practice unless there is a substantial difference between the shallow and deep time scales.

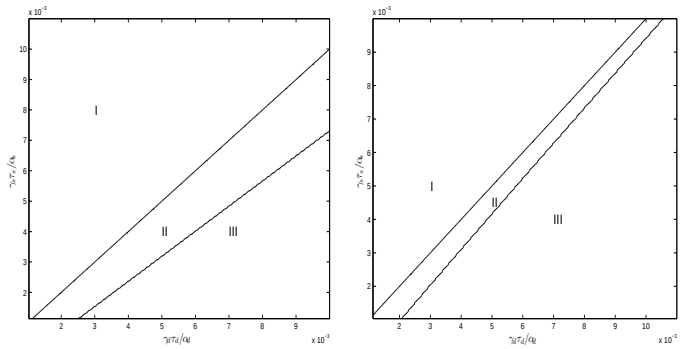


Figure 10: As in Fig. 6 but plotted for $\tau_s = 110$ s (left) and for $\tau_d = 110$ s (right), all other parameters remaining unchanged.

### 4.6.3 When $\tau_s \ll \tau_d$

Having established that a periodic solution does not occur for $\tau_s = \tau_d$ (Section 4.6.1) or for $\tau_s \approx \tau_d$ (Section 4.6.2), the natural next step in the analysis is to consider the behaviour of the system when these two time scales are well separated. In the present subsection, we consider $\tau_s \ll \tau_d$, and in the following subsection, we will consider $\tau_s \gg \tau_d$.

Starting from the eigenvalue equation as expressed by 51 and 52, the limit of $\tau_s \ll \tau_d$ can be considered by setting $\xi_s \simeq \sigma$ while retaining the full formula defining $\xi_d$. As a result, Eq. 52 reduces to

$$\sigma^2(2\sigma\tau_d + 1) + \hat{\gamma}_d\sigma - \hat{\gamma}_s\sigma(2\sigma\tau_d + 1) \simeq 0 \tag{80}$$

or

$$\sigma^2 + \frac{1}{2\tau_d}(1 - 2\tau_d\hat{\gamma}_s)\sigma + \frac{1}{2\tau_d}(\hat{\gamma}_d - \hat{\gamma}_s) \simeq 0 \tag{81}$$

which has the solution

$$4\tau_d\sigma \simeq -(1 - 2\tau_d\hat{\gamma}_s) \pm [(1 + \tau_d\hat{\gamma}_s)^2 - 8\tau_d\hat{\gamma}_d]^{1/2} \tag{82}$$

The solution is oscillatory when $8\tau_d\hat{\gamma}_d > (1 + \tau_d\hat{\gamma}_s)^2$, and it becomes purely oscillatory when $\tau_d\hat{\gamma}_s = 1/2$. Substituting the latter condition into the former we find that the conditions for a pure oscillation can be written as

$$\tau_d\hat{\gamma}_s = 1/2 \qquad \text{and} \qquad \hat{\gamma}_d < (9/16)\hat{\gamma}_s \tag{83}$$

Hence, the self–amplification rate, $\hat{\gamma}_s$, of shallow convection must balance with the self–dissipation rate, $\tau_d^{-1}$, of deep convection in order to obtain a purely oscillatory solution. Moreover, the self–dampening of deep convection through $\hat{\gamma}_d$ should not be too strong.

#### 4.6.4 When $\tau_s \gg \tau_d$

Now we briefly consider the opposite limit of $\tau_s \gg \tau_d$, repeating a similar procedure as in Section 4.6.3. The eigenvalue equation in this limit is

$$\sigma^2 + \frac{1}{2\tau_s}(1 + 2\tau_s\hat{\gamma}_d)\sigma + \frac{1}{2\tau_s}(\hat{\gamma}_d - \hat{\gamma}_s) \simeq 0 \tag{84}$$

which has the solution

$$4\tau_s\sigma \simeq -(1 + 2\tau_s\hat{\gamma}_d) \pm [(1 - \tau_s\hat{\gamma}_d)^2 + 8\tau_s\hat{\gamma}_s]^{1/2} \tag{85}$$

In this limit the eigenvalues are real for any choice of parameters.

### 4.7 The $p = 2$ equations with vanishing determinant: Periodic solution

In Section 4.6 we considered various special or approximate cases of the unforced coupled $p = 2$ system. An interesting form of solution that can arise is a periodic form, with the explosive and destructive tendencies of the system being offset against each other. Such a solution can only be obtained under a careful choice of the parameters: and, in particular, it does not occur for our default set described in Section 3.2. Here we consider what constraints on the parameters must be satisfied for a periodic solution. Unlike the previous subsection, we do not seek to understand the behaviour of the system in any limiting regime, but rather consider the general constraints.

Assuming a periodic solution, we can write $\sigma = i\omega$ where $\omega$ is real. Substituting this form into the eigenvalue equation 48, and equating the real and imaginary parts produces

$$\frac{-\omega^2}{2}\left(\frac{1}{\tau_d} + \frac{1}{\tau_s}\right) + \frac{1}{4\tau_d\tau_s}(\hat{\gamma}_d - \hat{\gamma}_s) = 0 \tag{86}$$

$$\omega^2 = \frac{\hat{\gamma}_d - \hat{\gamma}_s}{2(\tau_d + \tau_s)} \tag{87}$$

and

$$-\omega^3 + \frac{\omega}{4}\left[\frac{1}{\tau_d\tau_s} + 2\left(\frac{\hat{\gamma}_d}{\tau_d} - \frac{\hat{\gamma}_s}{\tau_s}\right)\right] = 0 \tag{88}$$

$$\omega^2 = \frac{1}{4}\left[\frac{1}{\tau_d\tau_s} + 2\left(\frac{\hat{\gamma}_d}{\tau_d} - \frac{\hat{\gamma}_s}{\tau_s}\right)\right] \tag{89}$$

respectively. Both equations for $\omega$ must be satisfied simultaneously to realize a periodic solution, which produces a constraint on the parameters.

$$\frac{\hat{\gamma}_d - \hat{\gamma}_s}{2(\tau_d + \tau_s)} = \frac{1}{4}\left[\frac{1}{\tau_d\tau_s} + 2\left(\frac{\hat{\gamma}_d}{\tau_d} - \frac{\hat{\gamma}_s}{\tau_s}\right)\right] \tag{90}$$

This can be rearranged to read

$$\tau_d^2\hat{\gamma}_s - \tau_s^2\hat{\gamma}_d = \frac{\tau_d + \tau_s}{2} \tag{91}$$

This is a necessary but not sufficient condition since it must be checked that the resulting $\omega$ is indeed real. From Eq. 87 this requires that $\hat{\gamma}_d > \hat{\gamma}_s$.

An interesting consequence of this condition can immediately be recognized. Rewriting Eq. 91 as

$$\hat{\gamma}_d = \left(\frac{\tau_d}{\tau_s}\right)^2 \hat{\gamma}_s - \left(\frac{\tau_d + \tau_s}{2\tau_s^2}\right) \tag{92}$$

it therefore follows that a periodic solution requires $\tau_d > \tau_s$.

It is straightforward to check that the general constraints of Eq. 91 and $\hat{\gamma}_d > \hat{\gamma}_s$ are consistent with the constraints previously derived for particular special cases and limits.

- For the case of $\tau_s = \tau_d = \tau$ as considered in Section 4.6.1, Eq. 91 gives $\hat{\gamma}_s - \hat{\gamma}_d = \tau^{-1}$ which violates the constraint $\hat{\gamma}_d > \hat{\gamma}_s$ and so there is no periodic solution.

- In the limit of $\tau_s \ll \tau_d$ as considered in Section 4.6.3, Eq. 91 immediately gives $\tau_d\hat{\gamma}_s = 1/2$ as derived previously.

- In the limit of $\tau_d \ll \tau_s$ as considered in Section 4.6.4, Eq. 91 immediately gives $\tau_s\hat{\gamma}_d = -1/2$ which cannot be satisfied and so there is no periodic solution.

## 4.8 Summary of results for the coupled $p = 2$ system

The system of Eqs. 13 and 14 arises from Arakawa and Schubert's (1974) energy cycle description for a system with two types of convection, along with Pan and Randall's (1998) assumption for the relationship between convective kinetic energy and cloud–base mass flux. All of the parameters in those equations are assumed to be positive in accordance with the arguments presented in Section 2.

The main results arising from our analysis of the system are that:

- The unforced shallow system is unstable in isolation (Section 4.1) whereas the unforced deep system in isolation has vanishing convective activity (Section 4.2).

- The coupled system may be unstable, damping or neutral according to the parameter settings. It may also exhibit periodicity. These possibilities were simply demonstrated for a limiting case where the mass fluxes equilibriate much more quickly than the cloud work function (Section 4.3).

- Solutions of particular interest are those for which the destabilizing and stabilizing tendencies of shallow and deep convection respectively are balanced. Such solution may still vary in time but they do not persistently grow or decay. A necessary condition for such a solution is that the determinant of the interaction matric $\mathcal{K}_{ij}$ should vanish (Section 4.4.1; Eq. 32).

- Assuming a vanishing determinant:

  - The solution takes the form of Eq. 42, with formulae for the coefficients being given in Section 4.5 and the cubic eigenfrequency equation being given in Eq. 48.
  - A necessary condition to avoid an exploding solution is that $\hat{\gamma}_d \geq \hat{\gamma}_s$ (Section 4.5; Eq. 50). If the solution does not explode, it will either decay towards an equilibrium configuration (possibly an oscillatory decay), or else it may produce persistent oscillations.
  - Persistent oscillations require the parameters to satisfy a further constraint, Eq. 91. They will not occur for $\tau_s = \tau_d$ (Section 4.6.1) or for $\tau_s \approx \tau_d$ (Section 4.6.2). They can only occur if $\tau_d > \tau_s$ (Sections 4.6.3, 4.6.4 and 4.7).

# 5 Analysis of the system: the $p = 1$ case

In Section 4 we investigated the energy-cycle system arising from the use of $p = 2$ in Eq. 5. As discussed in Section 3.1, the alternative of $p = 1$ is also an attractive possibility to consider, and doing so is the purpose of the present section. Setting $p = 1$ in Eq. 5 and substituting into Eqs. 3 and 4, the energy-cycle equations read

$$\dot{M}_s = \frac{M_s}{\tau_s}\left(\frac{A_s - A_{s0}}{A_{s0}}\right)$$

$$\dot{M}_d = \frac{M_d}{\tau_d}\left(\frac{A_d - A_{d0}}{A_{d0}}\right) \tag{93}$$

$$\dot{A}_s = \gamma_s M_s - \beta_d M_d + F_s$$

$$\dot{A}_d = \beta_s M_s - \gamma_d M_d + F_d \tag{94}$$

where

$$A_{s0} = \frac{\alpha_s}{\tau_s}$$

$$A_{d0} = \frac{\alpha_d}{\tau_d} \tag{95}$$

The analysis of the nonlinear $p = 1$ case in this section proceeds along similar lines as for the linear $p = 2$ case in the previous section. Thus, we begin by considering shallow and deep convection separately in Sections 5.1 and 5.2 respectively. The coupled system is considered in general terms in Sections 5.3 to 5.5 and its behaviour is exemplified by some useful linearizations presented in Sections 5.6 and 5.7. A summary of the results obtained is given in Section 5.8.

Since the $p = 1$ system is nonlinear, it is convenient to describe it in terms of nondimensional parameters from the outset, as seen below. We introduce the nondimensional couplings by

$$\hat{\gamma}_s = \frac{\gamma_s \tau_s^2 M_{s0}}{\alpha_s} = \frac{\gamma_s \tau_s M_{s0}}{A_{s0}} \qquad \hat{\beta}_s = \frac{\beta_s \tau_s \tau_d M_{s0}}{\alpha_d} = \frac{\beta_s \tau_s M_{s0}}{A_{d0}}$$

$$\hat{\gamma}_d = \frac{\gamma_d \tau_s \tau_d M_{d0}}{\alpha_d} = \frac{\gamma_d \tau_s M_{d0}}{A_{d0}} \qquad \hat{\beta}_d = \frac{\beta_d \tau_s^2 M_{d0}}{\alpha_s} = \frac{\beta_d \tau_s M_{d0}}{A_{s0}} \tag{96}$$

The reader should note that these rescaled coupling parameters are defined differently from Eq. 28 which introduced notation convenient for analysis of the $p = 2$ system. Since the $p = 2$ and $p = 1$ systems are analysed quite separately in this report there can be no scope for confusion. Here we have introduced arbitrary constants $M_{s0}$ and $M_{d0}$ to describe typical values of the mass fluxes for shallow and deep convection respectively. Rather than choosing values for these parameters, it is convenient to choose instead particular values for the nondimensional parameters $\hat{\gamma}_s$ and $\hat{\gamma}_d$ and then to use the definition of those parameters in order to set $M_{s0}$ and $M_{d0}$. Specifically we take

$$\hat{\gamma}_s = 1 \qquad \hat{\gamma}_d = 1 \tag{97}$$

so that

$$M_{s0} = \frac{\alpha_s}{\gamma_s \tau_s^2}$$

$$M_{d0} = \frac{\alpha_d}{\gamma_d \tau_s \tau_d} \tag{98}$$

and

$$\begin{aligned} \hat{\beta}_s &= \frac{\alpha_s \beta_s \tau_d}{\alpha_d \gamma_s \tau_s} \\ \hat{\beta}_d &= \frac{\alpha_d \beta_d \tau_s}{\alpha_s \gamma_d \tau_d} \end{aligned} \tag{99}$$

It is also convenient to define a parameter for the ratio of shallow and deep time scales,

$$\mu = \frac{\tau_s}{\tau_d} \tag{100}$$

Using the default parameter set discussed in Section 3.2 the parameters introduced in the present section take the values $M_{s0} = 10^{-2}$ kgm$^{-2}$s$^{-1}$, $M_{d0} = 5 \times 10^{-3}$ kgm$^{-2}$s$^{-1}$, $\hat{\beta}_s = 2$, $\hat{\beta}_d = 1/2$ and $\mu = 1$. These mass flux scalings are consistent with the typical values estimated by Yano and Plant (2012b).

## 5.1 Shallow convection only

The equations for the shallow mode only are (with dimensional variables)

$$\begin{aligned} \dot{M}_s &= \frac{M_s}{\tau_s} \left( \frac{A_s - A_{s0}}{A_{s0}} \right) \\ \dot{A}_s &= F_s + \gamma_s M_s. \end{aligned} \tag{101}$$

As before, we neglect any large-scale forcing of shallow convection so that $F_s = 0$. We also non-dimensionalize this system in terms of the scaling parameter for shallow mass flux, $M_{s0}$, that was introduced above, and the stationary value, $A_{s0}$ for the shallow cloud work function. Hence,

$$M_s = M_{s0} x_s, \qquad A_s = A_{s0}(1 + y_s) \tag{102}$$

so that $x_s$ and $y_s$ are the nondimensionalized mass flux and cloud work function respectively. We furthermore nondimensionalize time with $\tau_s$ to obtain

$$\begin{aligned} \dot{x}_s &= x_s y_s \\ \dot{y}_s &= \hat{\gamma}_s x_s \end{aligned} \tag{103}$$

using the nondimensional parameter $\hat{\gamma}_s$ defined above. These equations are further simplified by recalling that, without loss of generality, we set $\hat{\gamma}_s = 1$ above.

The shallow-only equations may be rewritten as

$$\frac{dx_s}{x_s y_s} = \frac{dy_s}{x_s} = d(t/\tau_s) \tag{104}$$

from which the first equality gives

$$dx_s = y_s dy_s. \tag{105}$$

This can be readily integrated to obtain the path of the system in phase space:

$$x_s = \frac{1}{2}(y_s^2 - y_s(0)^2) + x_s(0) \tag{106}$$

Substitution into the cloud work function equation leads to

$$\dot{y}_s = \frac{1}{2}(y_s^2 - y_s(0)^2) + x_s(0) \equiv \frac{1}{2}(y_s^2 - r_s^2) \tag{107}$$

Thus, the behaviour of the solution depends on the combination $r_s^2 \equiv y_s(0)^2 - 2x_s(0)$ from the initial conditions. For $r_s^2 < 0$ then the cloud work function must increase without limit, and likewise the mass flux will explode, as can be readily seen from its tendency equation. For $r_s^2 = 0$, we have

$$\dot{y}_s = \frac{1}{2}y_s^2 \tag{108}$$

which is easily integrated to give

$$y_s = \frac{2}{2/y_s(0) - (t/\tau_s)}. \tag{109}$$

In this case the cloud work function (and the mass flux) explode to infinity at $t = 2\tau_s/y_s(0)$ if its initial value is larger than the equilibrium value (*i.e.*, $y_s(0) > 0$) or else it approaches the equilibrium value (with vanishing mass flux) if the initial value is smaller than this. For $r_s^2 > 0$, the solution for the cloud work function is

$$y_s = -r_s \left[\left(\frac{y_s(0) - r_s}{y_s(0) + r_s}\right) e^{r_s t/\tau_s} + 1\right] \left[\left(\frac{y_s(0) - r_s}{y_s(0) + r_s}\right) e^{r_s t/\tau_s} - 1\right]^{-1} \tag{110}$$

In this case, the cloud work function tends to a stationary value of $-r_s$ as $t \to \infty$ times and its stationarity implies that the mass flux must vanish. Examples of exploding and decaying solutions of the unforced shallow equations are shown in Figs. 11 and 12 respectively.

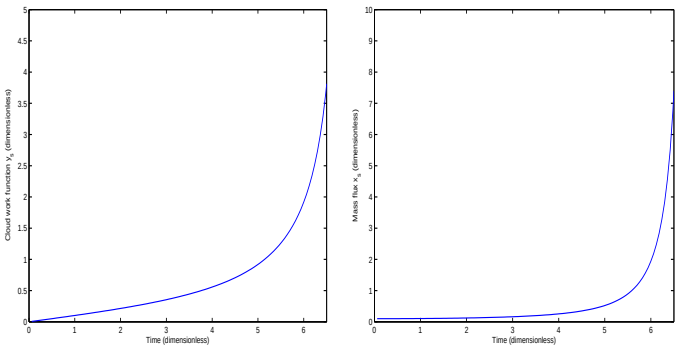


Figure 11: Solution for the unforced shallow mode alone in the $p = 1$ system. The parameters are the default set described in Section 3.2, giving scaling factors of $A_{s0} = 1$ Jkg$^{-1}$, $M_{s0} = 10^{-2}$ kgm$^{-2}$s$^{-1}$ and $\tau_s = 10^3$ s. The initial conditions are $x_s(0) = 0.1$, $y_s(0) = 0$ so that $r_s^2 = -0.2$. On the left and right respectively are shown the time series of the nondimensionalized cloud work function and of the nondimensionalized mass flux.

## 5.2 Deep convection only

The equations for the deep mode only are (with dimensional variables)

$$\begin{aligned} \dot{M}_d = &\quad \frac{M_d}{\tau_d}\left(\frac{A_d - A_{d0}}{A_{d0}}\right) \\ \dot{A}_d = &\quad F_d - \gamma_d M_d \end{aligned} \tag{111}$$

As before, we neglect any large-scale forcing of deep convection, $F_d = 0$. We also non-dimensionalize this system in terms of the scaling parameter for deep mass flux, $M_{d0}$, that was introduced above, and the stationary value, $A_{d0}$ for the deep cloud work function. Hence,

$$M_d = M_{d0} x_d, \qquad A_d = A_{d0}(1 + y_d) \tag{112}$$

so that $x_d$ and $y_d$ are the nondimensionalized mass flux and cloud work function respectively. Anticipating later analysis of the coupled system we furthermore nondimensionalize the time by using $\tau_s$ rather than $\tau_d$, to obtain

$$\begin{aligned} \dot{x}_d = &\quad \mu x_d y_d \\ \dot{y}_d = &\quad -\hat{\gamma}_d x_d \end{aligned} \tag{113}$$

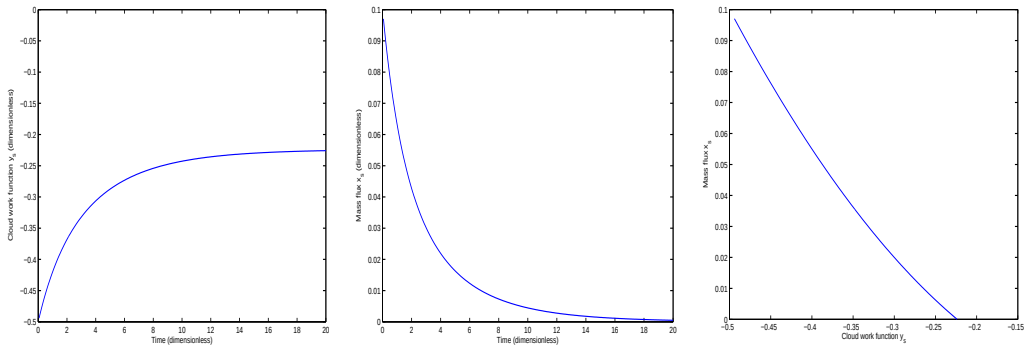


Figure 12: Solution for the unforced shallow mode alone in the $p = 1$ system. The parameters are the default set described in Section 3.2, giving scaling factors of $A_{s0} = 1$ Jkg$^{-1}$, $M_{s0} = 10^{-2}$ kgm$^{-2}$s$^{-1}$ and $\tau_s = 10^3$ s. The initial conditions are $x_s(0) = 0.1$, $y_s(0) = -0.5$ so that $r_s^2 = 0.05$. From left to right are shown: the time series of the nondimensionalized cloud work function, the time series of the nondimensionalized mass flux, and the trajectory in the phase space of the nondimensionalized cloud work function (horizontal axis) and the nondimensionalized mass flux (vertical axis).

using the nondimensional parameters defined above. These equations are further simplified by recalling that, without loss of generality, we set $\hat{\gamma}_d = 1$ above.

The deep-only equations may re–written as

$$\frac{dx_d}{\mu x_d y_d} = -\frac{dy_d}{x_d} = d(t/\tau_s) \tag{114}$$

As for the isolated shallow–convection system, the first equality can be readily integrated to give a phase–space solution,

$$x_d = -\frac{\mu}{2}(y_d^2 - y_d(0)^2) + x_d(0). \tag{115}$$

Substitution of the orbit equation into the cloud work function equation leads to

$$\dot{y}_d = -\frac{\mu}{2}(y_d^2 - y_d(0)^2) + x_d(0) \equiv -\frac{\mu}{2}(y_d^2 - r_d^2) \tag{116}$$

Thus, the behaviour of the solution depends on the combination $r_d^2 \equiv y_d(0)^2 + (2/\mu)x_d(0)$ from the initial conditions. This combination is guaranteed to be positive and the resulting cloud work function evolution is given

by

$$y_d = -r_d \left[1 + \left(\frac{y_d(0) - r_d}{y_d(0) + r_d}\right) e^{-\mu r_d t/\tau_s}\right] \left[1 - \left(\frac{y_d(0) - r_d}{y_d(0) + r_d}\right) e^{-\mu r_d t/\tau_s}\right]^{-1} \tag{117}$$

Thus, the cloud work function approaches $-r_d$ as $t \to \infty$. Substitution of this asymptotic tendency into the mass flux tendency equation shows that the mass flux vanishes as $t \to \infty$. Examples of numerical solutions to the unforced deep equations are shown in Figs. 13 and 14 for cases of initial growth or decay respectively.

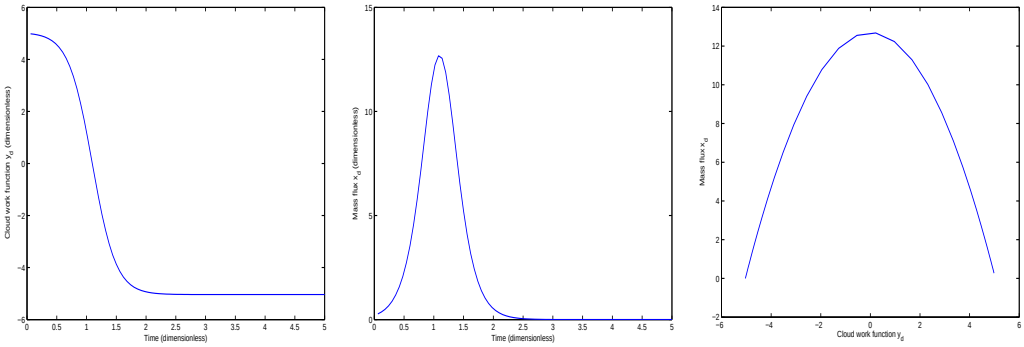


Figure 13: Solution for the unforced deep mode alone in the $p = 1$ system. The parameters are the default set described in Section 3.2, giving scaling factors of $A_{d0} = 10$ Jkg$^{-1}$, $M_{d0} = 5 \times 10^{-3}$ kgm$^{-2}$s$^{-1}$ and $\tau_s = 10^3$ s. The initial conditions are $x_d(0) = 0.2$, $y_s(0) = 5$ so that $r_d = 5.04$. Shown in the same format as in Fig. 12.

### 5.3 General case

We now proceed to discuss the coupled system of deep and shallow convection with $p = 1$. The relevant dimensional equations are given in Eqs. 93 and 94, and the forcings will again be set to zero. In terms of the dimensionless parameters and variables introduced by Eqs. 96–100, these equations read

$$\dot{x}_s = x_s y_s \tag{118}$$

$$\dot{x}_d = \mu x_d y_d \tag{119}$$

$$\dot{y}_s = x_s - \hat{\beta}_d x_d \tag{120}$$

$$\dot{y}_d = -x_d + \hat{\beta}_s x_s. \tag{121}$$

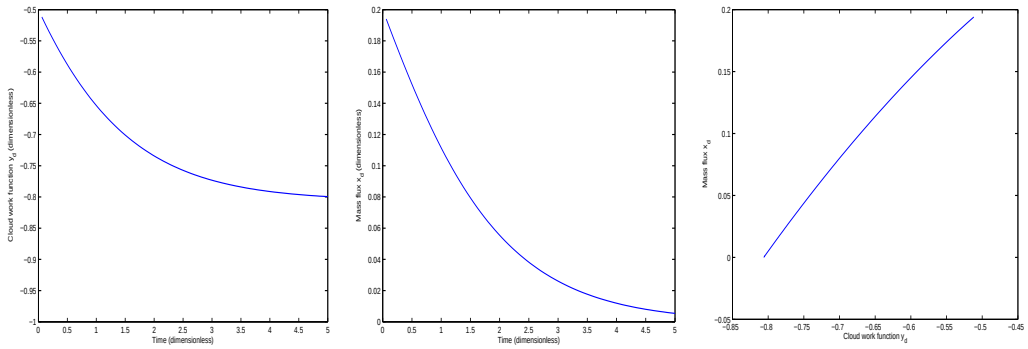


Figure 14: Solution for the unforced deep mode alone in the $p = 1$ system. The parameters are the default set described in Section 3.2, giving scaling factors of $A_{d0} = 10$ Jkg$^{-1}$, $M_{d0} = 5 \times 10^{-3}$ kgm$^{-2}$s$^{-1}$ and $\tau_s = 10^3$ s. The initial conditions are $x_d(0) = 0.2$, $y_s(0) = 5$ so that $r_d = -0.5$. Shown in the same format as in Fig. 12.

As with the coupled $p = 2$ system, our main interest is whether the possible explosive growth of shallow convection and the damping of deep convection can be coupled in such a way as to produce self–perpetuating behaviour, with deep convection acting as a break on shallow convection and shallow convection in turn providing a surrogate forcing for deep convection. Recalling Section 4.4.1, we first note that the condition of a vanishing determinant for the $\mathcal{K}_{ij}$ matrix is a prerequisite for such behaviour. Since this condition arises from the cloud work function equations alone, it applies regardless of the choice of $p$. The corresponding constraint on the parameters is as stated in Eq. 32. In non-dimensional units, it takes the form

$$\hat{\beta}_s \hat{\beta}_d = 1. \tag{122}$$

Asssuming a vanishing determinant, the cloud work function tendencies are then linked as in Eq. 35, or in non-dimensional units

$$\dot{y}_s = \hat{\beta}_d \dot{y}_d. \tag{123}$$

Accordingly, the cloud work functions themselves are linked by Eq. 36, or in non-dimensional units

$$y_s - y_s(0) = \hat{\beta}_d \left( y_d - y_d(0) \right). \tag{124}$$

Thus the cloud work functions for both modes evolve in phase for a vanishing determinant.

### 5.4 The $p = 1$ equations with vanishing determinant: General considerations

Using Eq. 124 (relating the cloud work functions) in Eq. 118 (the evolution equation for shallow mass flux) we find

$$\dot{x}_s = x_s y_s(0) + \hat{\beta}_d x_s \left(y_d - y_d(0)\right). \tag{125}$$

The deep cloud work function $y_d$ can then be eliminated by substituting from Eq. 119, the evolution equation for deep mass flux. The result is

$$\frac{\dot{x}_s}{x_s} = \frac{\hat{\beta}_d}{\mu}\frac{\dot{x}_d}{x_d} + y_s(0) - \hat{\beta}_d y_d(0) \tag{126}$$

Thus, in order to obtain a closed solution in phase space, an additional constraint on the initial conditions is required. Specifically, the initial cloud work functions must be related by

$$y_s(0) = \hat{\beta}_d y_d(0) \tag{127}$$

because otherwise the integration of Eq. 126 will produce a term proportional to time. We call this condition the *initial periodicity condition*. A consequence is that the two nondimensionalized cloud work functions are then proportional for all times, as can be seen from Eq. 124. Clearly the condition is satisfied if both cloud work functions start from their equilibrium values, $y_s(0) = y_d(0) = 0$.

A vanishing determinant and initial periodicity are necessary conditions for the periodicity of the solution to the coupled system, but they are not sufficient conditions. We investigate the system further below assuming the initial periodicity to hold. For the remainder of this subsection, however, we examine the character of the solutions when the initial periodicity condition is not met. In order to do so, it is convenient at this point to introduce some more notation, defining the dimensionless parameters

$$q = \frac{\hat{\beta}_d}{\mu} = \frac{\beta_d \alpha_d}{\gamma_d \alpha_s} \tag{128}$$

and

$$r_c = y_s(0) - \hat{\beta}_d y_d(0). \tag{129}$$

The initial periodicity condition corresponds to $r_c = 0$, while for the default parameters described in Section 3.2 we have $q = 1/2$. In terms of these parameters, Eq. 126 can be expressed as

$$\frac{\dot{x}_s}{x_s} = q\frac{\dot{x}_d}{x_d} + r_c. \tag{130}$$

Integration of the above equation gives

$$\frac{x_s}{x_s(0)} = \left(\frac{x_d}{x_d(0)}\right)^q e^{r_c(t/\tau_s)} \tag{131}$$

For $r_c > 0$ then $x_s \gg x_d$ as $t \to \infty$ so that deep convection becomes negligible and the system approaches the behaviour of the one-mode shallow-only system. As discussed in Section 5.1, that system may either explode or decay to zero activity. Likewise, for $r_c < 0$ then $x_s \ll x_d$ as $t \to \infty$ so that shallow convection becomes negligible and the system approaches the behaviour of the one-mode deep-only system. As discussed in Section 5.2 that system will always decay to zero activity. Examples of numerical solutions to the coupled equations for $r_c > 0$ and $r_c < 0$ are shown in Figs. 15 and 16 respectively.

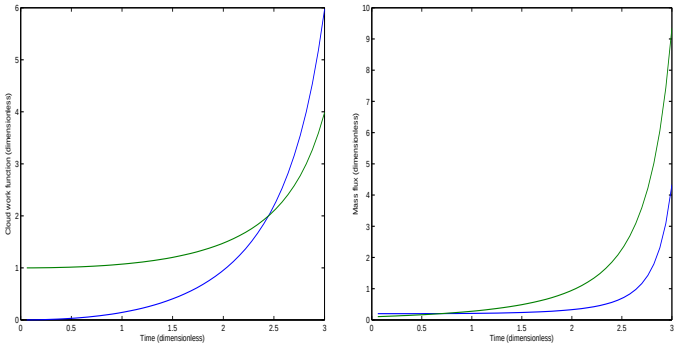


Figure 15: Solution for the unforced $p = 1$ system with parameters chosen to violate the initial periodicity condition. Blue is for the deep mode and green for the shallow mode. The parameters are the default set described in Section 3.2, giving scaling factors of $A_{d0} = 10$ Jkg$^{-1}$, $A_{s0} = 1$ Jkg$^{-1}$, $M_{d0} = 5 \times 10^{-3}$ kgm$^{-2}$s$^{-1}$, $M_{s0} = 10^{-2}$ kgm$^{-2}$s$^{-1}$ and $\tau_s = \tau_d = 10^3$ s. The initial conditions are $x_d(0) = 0.2$, $x_s(0) = 0.1$, $y_d(0) = 0$ and $y_s(0) = 1$ so that $r_c = 1$. Shown in the same format as in Fig. 11.

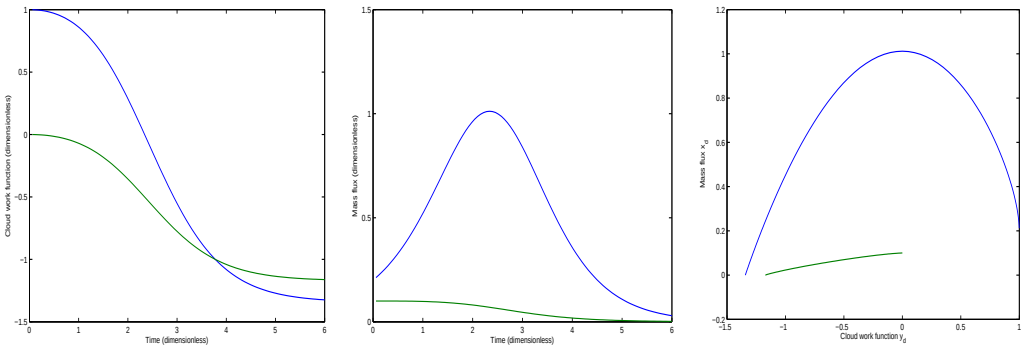


Figure 16: Solution for the unforced $p = 1$ system with parameters chosen to violate the initial periodicity condition. Blue is for the deep mode and green for the shallow mode. The parameters are the default set described in Section 3.2, giving scaling factors of $A_{d0} = 10$ Jkg$^{-1}$, $A_{s0} = 1$ Jkg$^{-1}$, $M_{d0} = 5 \times 10^{-3}$ kgm$^{-2}$s$^{-1}$, $M_{s0} = 10^{-2}$ kgm$^{-2}$s$^{-1}$ and $\tau_s = \tau_d = 10^3$ s. The initial conditions are $x_d(0) = 0.2$, $x_s(0) = 0.1$, $y_d(0) = 1$ and $y_s(0) = 0$ so that $r_c = -0.5$. Shown in the same format as in Fig. 12.

## 5.5 Behaviour of the system with initial periodicity conditions

We now consider the character of the solution assuming both a vanishing determinant and the initial periodicity condition, $r_c = 0$. The key issue here is to identify whether any additional conditions are required in order to obtain a periodic solution.

When initial periodicity holds, the relationship between shallow and deep mass flux in Eq. 131 reduces to

$$\frac{x_s}{x_s(0)} = \left(\frac{x_d}{x_d(0)}\right)^q \tag{132}$$

The path of the solution in phase space can also be derived for the other variables. For example, a solution in terms of the deep variables $x_d, y_d$ can be obtained by first substituting for $x_s$ from Eq. 132 into Eq. 121 to obtain a differential equation containing $x_d$ and $y_d$. Combining that with Eq. 119 we can then eliminate the time to obtain a differential equation connecting $x_d$ and $y_d$. Integrating the resulting equation produces

$$\frac{\mu y_d^2}{2} + x_d - \frac{\hat{\beta}_s}{q} x_s(0) \left(\frac{x_d}{x_d(0)}\right)^q = \frac{\mu y_d(0)^2}{2} + x_d(0) - \frac{\hat{\beta}_s}{q} x_s(0) \tag{133}$$

Similarly it is straightforward to find the solution path in the shallow part of phase space to be

$$\frac{y_s^2}{2} - x_s + \hat{\beta}_d q x_d(0) \left(\frac{x_s}{x_s(0)}\right)^{1/q} = \frac{y_s(0)^2}{2} - x_s(0) + \hat{\beta}_d q x_d(0) \tag{134}$$

Together Eqs. 132, 133 and 134 describe the complete solution in phase space. We now consider the form of that solution. In order to do so we examine below the solution in the phase space of the deep variables. An analysis in terms of the shallow variables has been performed along very similar lines and is entirely consistent with the conclusions reached below.

We first define the function

$$X_d(x_d) = x_d - \frac{\hat{\beta}_s}{q} x_s(0) \left(\frac{x_d}{x_d(0)}\right)^q \tag{135}$$

and the constant

$$u_d = \mu \frac{y_d(0)^2}{2} + x_d(0) - \frac{\hat{\beta}_s}{q} x_s(0) \tag{136}$$

so that Eq. 133 reads

$$\mu \frac{y_d^2}{2} + X_d(x_d) = u_d. \tag{137}$$

An extreme value for $X_d$ occurs at

$$x_d^{\text{ex}} = \left(\frac{x_d(0)^q}{\hat{\beta}_s x_s(0)}\right)^{1/(q-1)} \tag{138}$$

at which point

$$X_d(x_d^{\text{ex}}) = \left(1 - \frac{1}{q}\right) \left[\frac{x_d(0)^q}{\hat{\beta}_s x_s(0)}\right]^{1/(q-1)} \tag{139}$$

To see what kind of extreme value this is, we can look at the second derivative

$$\frac{d^2 X_d}{dx_d^2} = -(q-1) \frac{\hat{\beta}_s x_s(0) x_d^{q-2}}{x_d(0)^q} \tag{140}$$

Thus, the form of the solution depends on $q$ with three possibilities to be considered further in the following three subsections: $q > 1$ in which case $X_d$ has a maximum, $q = 1$ in which case $X_d$ is unbounded, and $q < 1$ in which case $X_d$ has a minimum. From Eq. 137 we immediately notice that for $y_d^2$ to be bounded then $X_d$ must have a minimum. Thus, if $q < 1$ then we ensure a solution that cannot explode. Examples and further discussions are given below.

### 5.5.1 Form of solution for $q > 1$

If $q > 1$ then $X_d$ has a maximum at a positive value of $X_d$ as sketched in Fig. 17 (on the left).

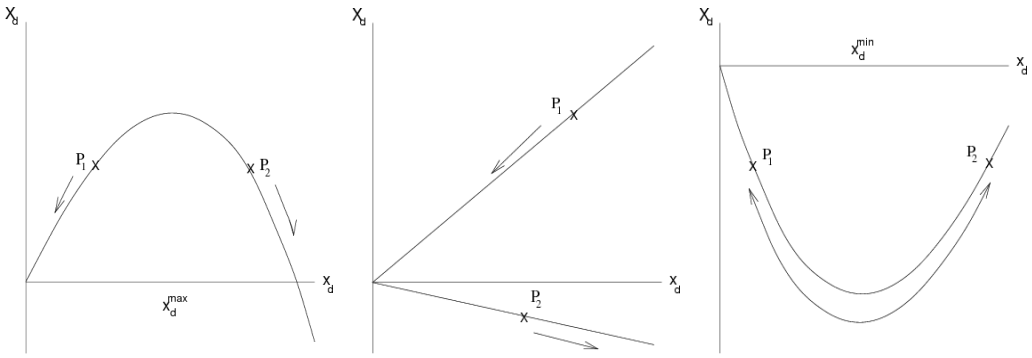


Figure 17: Sketch of the function $X_d(x_d)$ for (left) $q > 1$, (center) $q = 1$ and (right) $q < 1$.

Consider the point P at which $y_d = 0$ in the phase space of $(x_d, X_d)$. Here $X_d$ has its maximum value that could be obtained in an actual solution of Eq. 137, with $X_d(x_d) = u_d$. This point could correspond to the maximum possible value of the function $X_d(x_d)$ as determined above, but more likely is that there are two possible solutions, P, for $X_d(x_d) = u_d$ on either side of that maximum. We label those points as $P_1$ and $P_2$ on the left and right of the maximum respectively. Which side of the $X_d(x_d)$ curve an actual solution remains will depend upon the initial conditions.

Suppose that we are initially on the left-hand branch of the curve (*i.e.*, if $x_d(0) < x_d^{\rm ex}$). Any value of $y_d \neq 0$ that occurs in the solution must correspond to a smaller value of $x_d$ compared to that at $P_1$. This means that the solution can only occupy the region between $P_1$ and the origin, thus including the possibilty of $x_d \to 0$ (and also $x_s \to 0$) so that all convective activity dies out. Fig. 18 illustrates a numerical solution.

Otherwise the initial state may be on the right-hand branch of the $X_d(x_d)$ curve (*i.e.*, with $x_d(0) > x_d^{\rm ex}$). In that case any value of $y_d \neq 0$ that occurs in the solution must correspond to a larger value of $x_d$ compared to that at $P_2$. This means that the solution occupies a region between $P_2$ and a point where $x_d \to \infty$ (and also $x_s \to \infty$). Thus the system is able to explode. Fig. 19 illustrates a numerical solution for this case.

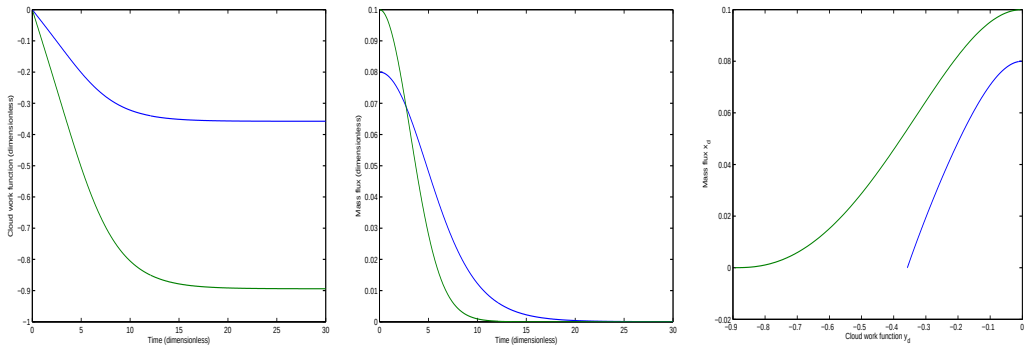


Figure 18: Solution for the unforced $p = 1$ system with $q > 1$. Blue is for the deep mode and green for the shallow mode. The parameters are the default set described in Section 3.2 except for $\alpha_d = 5 \times 10^4$ m$^2$ s$^{-1}$, giving scaling factors of $A_{d0} = 50$ Jkg$^{-1}$, $A_{s0} = 1$ Jkg$^{-1}$, $M_{d0} = 2.5 \times 10^{-2}$ kgm$^{-2}$s$^{-1}$, $M_{s0} = 10^{-2}$ kgm$^{-2}$s$^{-1}$ and $\tau_s = \tau_d = 10^3$ s. The parameter $q = 2.5$. The initial conditions are $x_d(0) = 0.08$, $x_s(0) = 0.1$, $y_d(0) = 0$ and $y_s(0) = 0$ so that $r_c = 0$. The maximum of $X_d(x_d)$ occurs for $x_d^{\rm ex} = 0.127$. Shown in the same format as in Fig. 12.

### 5.5.2 Form of solution for $q = 1$

If $q = 1$ then $X_d$ becomes simply proportional to $x_d$ and so the function does not have any extreme values. A sketch of the situation can be seen in Fig. 17 (in the centre). Specifically, we have

$$X_d = x_d \left[ 1 - \frac{\hat{\beta}_s}{q} \frac{x_s(0)}{x_d(0)} \right] \tag{141}$$

According to the sign of the factor in square brackets, $X_d$ is a straight line through the origin with either positive or negative gradient.

Consider the case of a positive gradient (*i.e.*, if $q x_d(0) > \hat{\beta}_s x_s(0)$) and a point $\mathrm{P}_1$ in the phase space of $(x_d, X_d)$ at which $y_d = 0$ and so $X_d(x_d) = u_d$. This is the maximum value of $X_d$ that can be obtained in an actual solution to our system and any other value of $y_d$ that occurs must therefore correspond to a smaller value of $x_d$ compared to that at $\mathrm{P}_1$. This means that the solution can reach a situation where $x_d \to 0$ (and also $x_s \to 0$) so that all convective activity dies out. Fig. 20 illustrates this case numerically.

For the case of a negative gradient, we consider a point $\mathrm{P}_2$, again defined

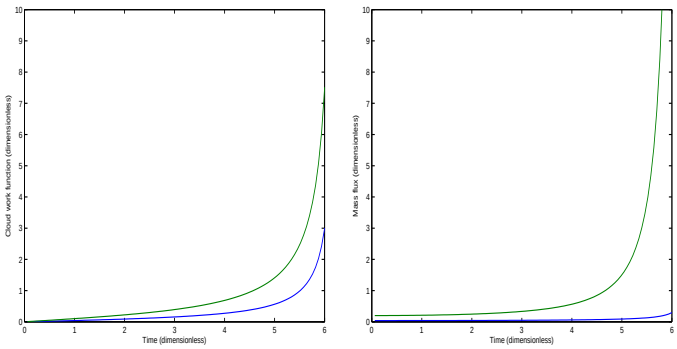


Figure 19: Solution for the unforced $p = 1$ system with $q > 1$. Blue is for the deep mode and green for the shallow mode. The parameters are the default set described in Section 3.2 except for $\alpha_d = 5 \times 10^4$ m$^2$ s$^{-1}$, giving scaling factors of $A_{d0} = 50$ Jkg$^{-1}$, $A_{s0} = 1$ Jkg$^{-1}$, $M_{d0} = 2.5 \times 10^{-2}$ kgm$^{-2}$s$^{-1}$, $M_{s0} = 10^{-2}$ kgm$^{-2}$s$^{-1}$ and $\tau_s = \tau_d = 10^3$ s. The parameter $q = 2.5$. The initial conditions are $x_d(0) = 0.04$, $x_s(0) = 0.1$, $y_d(0) = 0$ and $y_s(0) = 0$ so that $r_c = 0$. The maximum of $X_d(x_d)$ occurs for $x_d^{\rm ex} = 0.025$. Shown in the same format as in Fig. 11.

by $y_d = 0$ and $X_d(x_d) = u_d$. In this case any other value of $y_d$ that occurs in the solution must make $X_d$ more negative and must therefore correspond to a larger value of $x_d$ compared to that at $\mathrm{P}_2$. Thus the system is able to explode. Fig. 21 illustrates this case numerically.

### 5.5.3 Form of solution for $q < 1$

If $q < 1$ then $X_d$ has a minimum at a negative value of $X_d$. A sketch of the situation can be seen in Fig. 17 (on the right).

Once again we consider a point P in the phase space of $(x_d, X_d)$ given by $y_d = 0$ and hence $X_d(x_d) = u_d$. The point could correspond to the minimum of the function $X_d(x_d)$ as derived above, but more likely is that there are two possible solutions for P on either side of that minimum. We label those points as $\mathrm{P}_1$ and $\mathrm{P}_2$ on the left and right of the minimum respectively.

Suppose that the initial conditions place us on the $\mathrm{P}_1$ side of the curve (*i.e.*, if $x_d(0) < x_d^{\rm ex}$). Any non-zero value of $y_d$ that occurs in the solution must correspond to a larger value of $x_d$ compared to that at $\mathrm{P}_1$. This means that the solution can access the $\mathrm{P}_2$ side of the curve although it cannot go

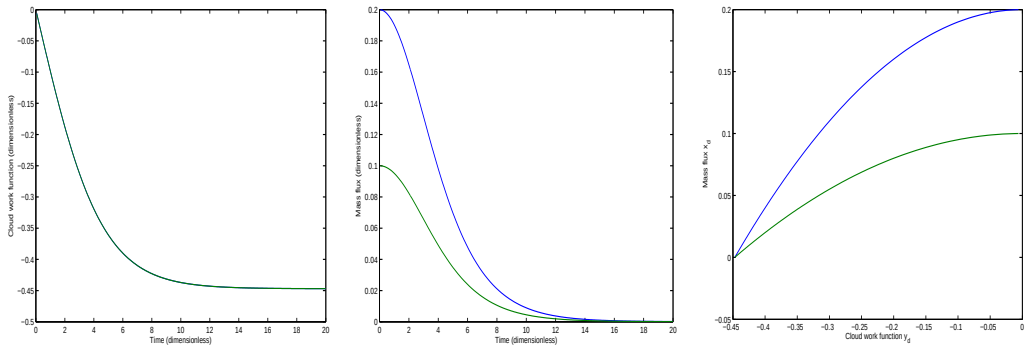


Figure 20: Solution for the unforced $p = 1$ system with $q = 1$. Blue is for the deep mode and green for the shallow mode. The parameters are the default set described in Section 3.2 except for $\alpha_d = 2 \times 10^4$ m$^2$ s$^{-1}$, giving scaling factors of $A_{d0} = 20$ Jkg$^{-1}$, $A_{s0} = 1$ Jkg$^{-1}$, $M_{d0} = 10^{-2}$ kgm$^{-2}$s$^{-1}$, $M_{s0} = 10^{-2}$ kgm$^{-2}$s$^{-1}$ and $\tau_s = \tau_d = 10^3$ s. The initial conditions are $x_d(0) = 0.2$, $x_s(0) = 0.1$, $y_d(0) = 0$ and $y_s(0) = 0$ so that $r_c = 0$. Shown in the same format as in Fig. 12.

beyond the point $P_2$ itself because there are no values of $y_d$ that could allow it.

Otherwise, for initial conditions on the $P_2$ side of the curve, any non-zero value of $y_d$ that occurs corresponds to a smaller value of $x_d$ compared to that at $P_2$. This means that the solution can access the $P_1$ side of the curve although of course we cannot go past the point $P_1$ itself. Fig. 22 illustrates the periodic solution that is found numerically for $q < 1$.

### 5.6 Linearization of the $p = 1$ system

The $p = 1$ system is fully nonlinear as emphasized by Yano and Plant (2012a) for the one–mode case. It is nonetheless revealing to consider linear analyses to study the evolution in the vicinity of various situations of particular interest. Important questions concern the behaviour of the system when it deviates slightly from the full set of conditions for periodicity that were determined in Sections 5.3 to 5.5. After presenting a linear formulation in Section 5.6.1 below, we then consider a range of special cases in turn.

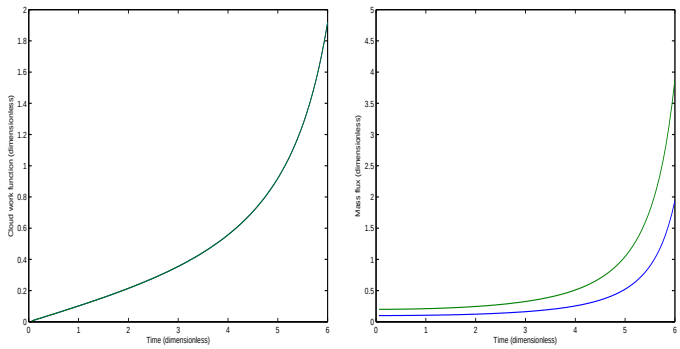


Figure 21: Solution for the unforced $p = 1$ system with $q = 1$. Blue is for the deep mode and green for the shallow mode. The parameters are the default set described in Section 3.2 except for $\alpha_d = 2 \times 10^4$ m$^2$ s$^{-1}$, giving scaling factors of $A_{d0} = 20$ Jkg$^{-1}$, $A_{s0} = 1$ Jkg$^{-1}$, $M_{d0} = 10^{-2}$ kgm$^{-2}$s$^{-1}$, $M_{s0} = 10^{-2}$ kgm$^{-2}$s$^{-1}$ and $\tau_s = \tau_d = 10^3$ s. The initial conditions are $x_d(0) = 0.1$, $x_s(0) = 0.2$, $y_d(0) = 0$ and $y_s(0) = 0$ so that $r_c = 0$. Shown in the same format as in Fig. 11.

### 5.6.1 General approach for linearization with vanishing determinant

Consider a linearization of the coupled $p = 1$ system about an arbitrary reference state, which we will denote by using a subscript $r$. If the departure from the reference state is denoted using a prime then the linearized form of the coupled Eqs. 118 to 121 becomes

$$\dot{x}'_s = x_{sr} y'_s + y_{sr} x'_s \tag{142}$$
$$\dot{x}'_d = \mu(x_{dr} y'_d + y_{dr} x'_d) \tag{143}$$
$$\dot{y}'_s = x_{sr} - \hat{\beta}_d x_{dr} + x'_s - \hat{\beta}_d x'_d \tag{144}$$
$$\dot{y}'_d = -x_{dr} + \hat{\beta}_s x_{sr} - x'_d + \hat{\beta}_s x'_s \tag{145}$$

We specialize to reference states that satisfy

$$x_{sr} = \hat{\beta}_d x_{dr} \tag{146}$$
$$x_{dr} = \hat{\beta}_s x_{sr}. \tag{147}$$

The combination of these two constraints means that $\hat{\beta}_s \hat{\beta}_d = 1$ and so we are dealing with a vanishing determinant as discussed in Section 5.3. This means

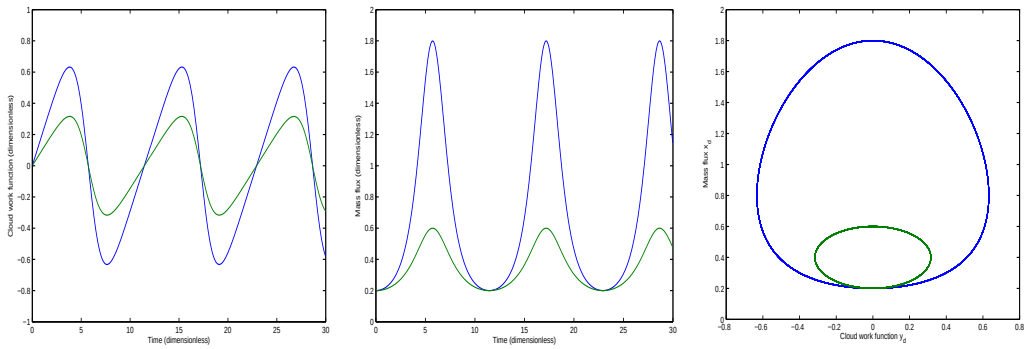


Figure 22: Solution for the unforced $p = 1$ system with $q < 1$. Blue is for the deep mode and green for the shallow mode. The parameters are the default set described in Section 3.2, giving scaling factors of $A_{d0} = 20$ Jkg$^{-1}$, $A_{s0} = 1$ Jkg$^{-1}$, $M_{d0} = 10^{-2}$ kgm$^{-2}$s$^{-1}$, $M_{s0} = 10^{-2}$ kgm$^{-2}$s$^{-1}$ and $\tau_s = \tau_d = 10^3$ s. The initial conditions are $x_d(0) = 0.2$, $x_s(0) = 0.2$, $y_d(0) = 0$ and $y_s(0) = 0$ so that $r_c = 0$. The parameter $q = 0.5$. Shown in the same format as in Fig. 12.

that the cloud–work functions are linked by Eq. 124, and by furthermore taking the initial state to be the reference state this reads

$$y'_s = \hat{\beta}_d y'_d. \tag{148}$$

Since the above relation must be satisfied at all times, this includes the initial time, and so the reference state must itself satisfty the initial periodicity condition,

$$y_{sr} = \hat{\beta}_d y_{dr}. \tag{149}$$

Although this constraint and Eq. 146 mean that reference state is not arbitrary it should be recognized that there is still considerable freedom remaining in its choice. Using Eq. 148 to eliminate $y'_d$, Eqs. 142 to 144 become

$$\left(\frac{d}{dt} - y_{sr}\right) x'_s = x_{sr} y'_s \tag{150}$$

$$\left(\frac{d}{dt} - \frac{y_{sr}}{q}\right) x'_d = \frac{x_{sr}}{\mu q^2} y'_s \tag{151}$$

$$\dot{y}'_s = x'_s - \mu q x'_d \tag{152}$$

where we have also made use of Eqs. 146 and 148 to eliminate $x_{dr}$ and $y_{dr}$ respectively and have expressed the final result using the parameter $q$ defined in Eq. 128. From the above equations we can now easily derive an eigenvalue equation. Specifically, Eq. 152 gives

$$\sigma y'_s = x'_s - \mu q x'_d \tag{153}$$

such that by eliminating $y'_s$ Eqs. 150 and 151 become

$$\left[\sigma(\sigma - y_{sr}) - x_{sr}\right] x'_s + \mu q x_{sr} x'_d = 0 \tag{154}$$

and

$$\left[\sigma\left(\sigma - \frac{y_{sr}}{q}\right) + \frac{x_{sr}}{q}\right] x'_d - \frac{x_{sr}}{\mu q^2} x'_s = 0 \tag{155}$$

respectively. Now by taking the determinant of the above two equations, we obtain the eigenvalue equation

$$\sigma^2 - \frac{y_{sr}}{q}(1+q)\sigma + \frac{1}{q}\left(x_{sr}(1-q) + y_{sr}^2\right) = 0 \tag{156}$$

This is the statement of the eigenvalue problem for a linearization of the coupled $p = 1$ system about an initial reference state for which the conditions 146 and 147 hold. We consider two possible choices of reference state in the next subsections.

### 5.6.2 Reference state 1: Linearization about zero mass flux

For a linearization about zero mass flux we set $x_{sr} = x_{dr} = 0$ so that the cubic eigenvalue equation 156 reduces to

$$\sigma^2 - \frac{y_{sr}}{q}(1+q)\sigma + \frac{1}{q} y_{sr}^2 = 0 \tag{157}$$

with roots $\sigma = y_{sr}$ and $y_{sr}/q$. Thus, the modes are either both growing or both decaying according to the sign of the anomalous cloud work function. The result accords with the physical expectation that from an initial state of zero mass flux then excess of cloud work function beyond the equilibrium value will lead to the growth of convection, whereas a reduction below equilibrium will produce decay of any linear fluctuation.

Figs. 23 and 24 show example results for this approximation with $y_{sr}$ positive and negative respectively. The plots include the solution obtained from the fully nonlinear equations as well as that from the linearized equation set. The two solutions agree very well, up to $t \sim 3\tau_s$ in the former case and at all times in the latter case.

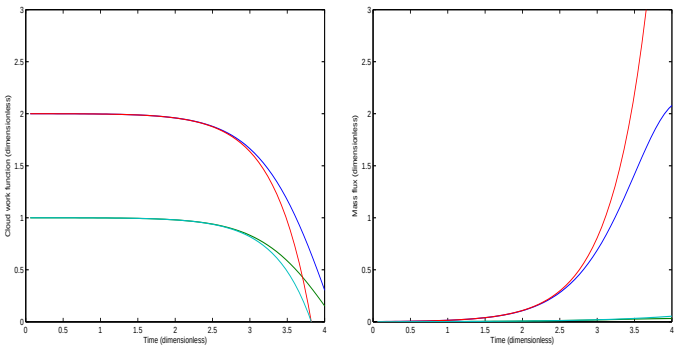


Figure 23: Numerical example solution for a linearized approximation of the unforced $p = 1$ system. The parameters are the default set described in Section 3.2, giving scaling factors of $A_{d0} = 20$ Jkg$^{-1}$, $A_{s0} = 1$ Jkg$^{-1}$, $M_{d0} = 10^{-2}$ kgm$^{-2}$s$^{-1}$, $M_{s0} = 10^{-2}$ kgm$^{-2}$s$^{-1}$ and $\tau_s = \tau_d = 10^3$ s. The initial conditions are $x_d(0) = 2\times10^{-3}$, $x_s(0) = 10^{-3}$, $y_d(0) = 2$ and $y_s(0) = 1$. Blue is for the deep mode and green for the shallow mode using the fully nonlinear equations. Red is for the deep mode and cyan for the shallow mode using the linearized equations described in Section 5.6.1 and a reference state of $x_{sr} = x_{dr} = 0$. Shown in the same format as in Fig. 11.

### 5.6.3 Reference state 2: Linearization about cloud work function equilibrium

Equilibrium of the mass flux tendency equations, 118 and 119, occurs when the cloud work functions are $y_s = y_d = 0$ respectively. Linearizing about that state reduces the eigenvalue equation 156 to

$$\sigma^2 = \left(\frac{q-1}{q}\right) x_{sr} \tag{158}$$

Thus, a linear perturbation about the cloud work function equilibrium state is exponentially growing for $q > 1$ and oscillatory for $q < 1$, consistent with the nonlinear analysis of Section 5.5. Figs. 25 and 26 show example results for this linear regime with $q > 1$ and $q < 1$ respectively.

An interesting point to notice is that the square of the oscillation frequency (assuming $q < 1$) is proportional to the reference/initial state mass flux, here written in terms of shallow convection. Thus, the period of oscillation could be arbitrarily increased by decreasing the initial amplitude

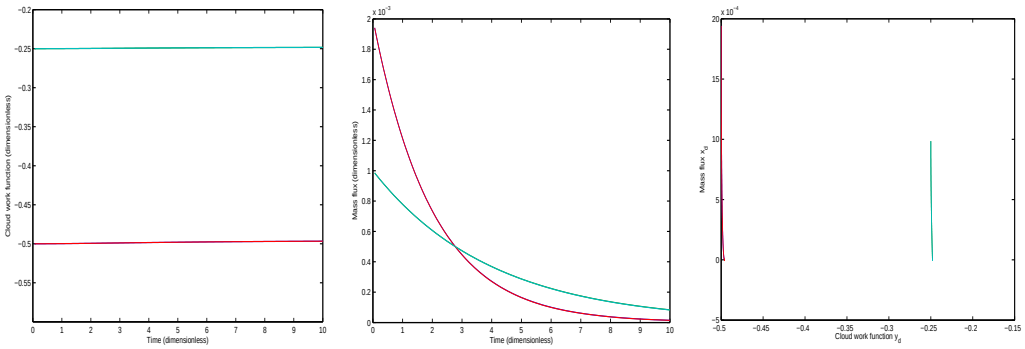


Figure 24: Numerical example solution for a linearized approximation of the unforced $p = 1$ system. The parameters are the default set described in Section 3.2, giving scaling factors of $A_{d0} = 20$ Jkg$^{-1}$, $A_{s0} = 1$ Jkg$^{-1}$, $M_{d0} = 10^{-2}$ kgm$^{-2}$s$^{-1}$, $M_{s0} = 10^{-2}$ kgm$^{-2}$s$^{-1}$ and $\tau_s = \tau_d = 10^3$ s . The initial conditions are $x_d(0) = 2 \times 10^{-3}$, $x_s(0) = 10^{-3}$, $y_d(0) = -0.5$ and $y_s(0) = -0.25$. Blue is for the deep mode and green for the shallow mode using the fully nonlinear equations. Red is for the deep mode and cyan for the shallow mode using the linearized equations described in Section 5.6.1 and a reference state of $x_{sr} = x_{dr} = 0$. Shown in the same format as in Fig. 12.

of convective activity. In principle, the oscillation period could even be extended to an MJO time scale.

Let us now extend the above analysis by supposing the reference state to be a small departure from the cloud work function equilibrium. We set $y_{sr} = \epsilon$ and expand the eigenvalue equation 156 in powers of $\epsilon$. Writing the eigenvalues as $\sigma \approx \sigma_0 + \sigma_1$ with $\sigma_0$ given by Eq. 158 and $\sigma_1$ being linear in $\epsilon$, the eigenvalue equation reads

$$2\sigma_0\sigma_1 - (1+q)\frac{\epsilon}{q}\sigma_0 = 0. \tag{159}$$

at first order in $\epsilon$. This may be rearranged to give

$$\sigma_1 = \frac{1+q}{2q}\epsilon \tag{160}$$

Thus, the effect of this correction depends on the sign of the departure from the cloud work function equilibrium value. A slight excess (deficit) of the

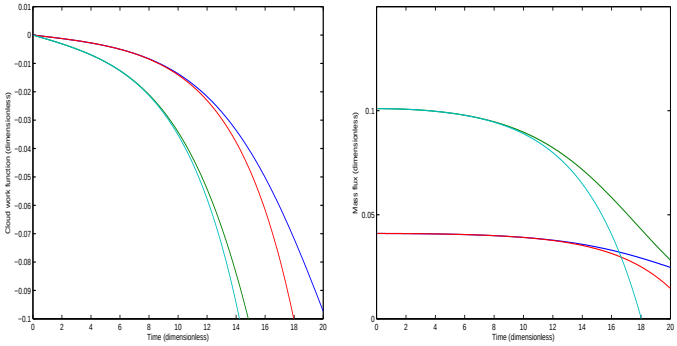


Figure 25: Numerical example solution for a linearized approximation of the unforced $p = 1$ system. The parameters are the default set described in Section 3.2, except for $\alpha_d = 5 \times 10^{-4}\text{m}^2\text{s}^{-1}$, giving scaling factors of $A_{d0} = 50$ Jkg$^{-1}$, $A_{s0} = 1$ Jkg$^{-1}$, $M_{d0} = 2.5 \times 10^{-2}$ kgm$^{-2}$s$^{-1}$, $M_{s0} = 10^{-2}$ kgm$^{-2}$s$^{-1}$ and $\tau_s = \tau_d = 10^3$ s. The parameter $q = 2.5$. The initial conditions are $x_d(0) = 0.041$, $x_s(0) = 0.101$, $y_d(0) = 0$ and $y_s(0) = 0$. Blue is for the deep mode and green for the shallow mode using the fully nonlinear equations. Red is for the deep mode and cyan for the shallow mode using the linearized equations described in Section 5.6.1 and a reference state of $x_{sr} = 0.04$, $x_{dr} = 0.1$, $y_{sr} = y_{dr} = 0$. Shown in the same format as in Fig. 11.

cloud work function increases (decreases) the growth rate for the $q > 1$ case and produces a slowly growing (decaying) aspect to the oscillatory solution for $q < 1$. A numerical example of the correction in an oscillatory case is shown in Fig. 27.

### 5.6.4 Linearization with a time scale separation

The above numerical examples were for cases where $\mu = 1$ and showed that the linearized equations are able to give a good approximation to the full system, at least for times $t$ of order a few $\tau_s$. However, it should be noted that a linearization works less well if there is a time scale separation.

Suppose first that shallow convection is damped very slowly compared to deep convection so that $\tau_s \gg \tau_d$, or in other words $\mu \gg 1$. In this limit shallow convection dominates and the system quickly comes to resemble the shallow-only regime which is markedly nonlinear. Longer integrations with

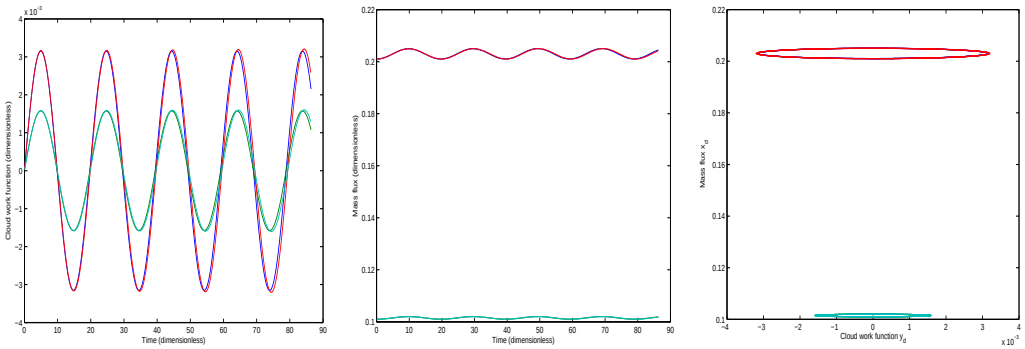


Figure 26: Numerical example solution for a linearized approximation of the unforced $p = 1$ system. The parameters are the default set described in Section 3.2, giving scaling factors of $A_{d0} = 20$ Jkg$^{-1}$, $A_{s0} = 1$ Jkg$^{-1}$, $M_{d0} = 10^{-2}$ kgm$^{-2}$s$^{-1}$, $M_{s0} = 10^{-2}$ kgm$^{-2}$s$^{-1}$ and $\tau_s = \tau_d = 10^3$ s. The parameter $q = 0.5$. The initial conditions are $x_d(0) = 0.201$, $x_s(0) = 0.101$, $y_d(0) = 0$ and $y_s(0) = 0$. Blue is for the deep mode and green for the shallow mode using the fully nonlinear equations. Red is for the deep mode and cyan for the shallow mode using the linearized equations described in Section 5.6.1 and a reference state of $x_{sr} = 0.1$, $x_{dr} = 0.2$, $y_{sr} = y_{dr} = 0$. Shown in the same format as in Fig. 12.

$q < 1$ confirm that deep convection can tame this growth tendency and produce the oscillating solution expected but clearly such behaviour is only apparent for the full nonlinear system. Fig. 28 illustrates these points.

In the opposite limit of $\mu \ll 1$ shallow convection is rapidly damped compared to deep convection. Here again, numerical tests of the linearized system perform relatively poorly. Fig. 29 gives an illustration. In order for linearity to be a good approximation we require the deep and shallow modes to be well balanced at all times, while the fully nonlinear equation set is needed to handle a situation where one of the modes dominates the instantaneous dynamics.

## 5.7 Linearization for the case of a non-zero determinant

We now return to the linearized equations 142 to 145 but develop these in a different way. In Section 5.6.1 we restricted attention to reference states satisfying Eqs. 146 and 147, thereby commiting to the case of a vanishing

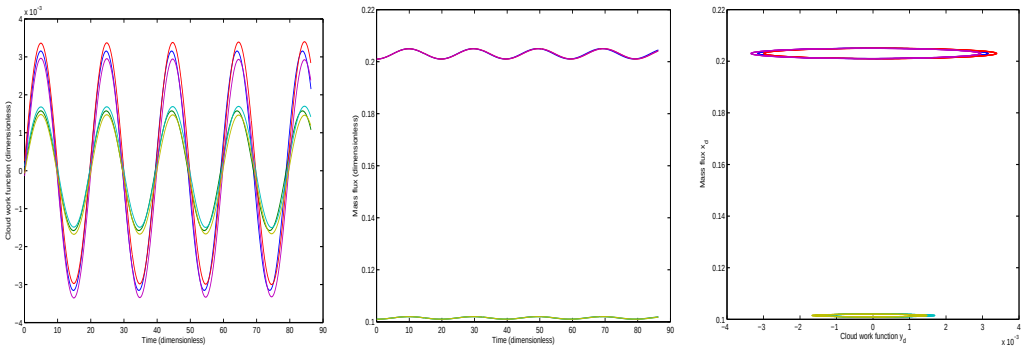


Figure 27: Numerical example solution for a linearized approximation of the unforced $p = 1$ system. The parameters are the default set described in Section 3.2 giving scaling factors of $A_{d0} = 16.67$ Jkg$^{-1}$, $A_{s0} = 1$ Jkg$^{-1}$, $M_{d0} = 8.3 \times 10^{-3}$ kgm$^{-2}$s$^{-1}$, $M_{s0} = 10^{-2}$ kgm$^{-2}$s$^{-1}$ and $\tau_s = 10^3$ s. The parameter $q = 0.5$. The initial conditions are $x_d(0) = 0.201$, $x_s(0) = 0.101$, $y_d(0) = \epsilon$ and $y_s(0) = 2\epsilon$. Blue is for the deep mode and green for the shallow mode with $\epsilon = 0$. Red is for the deep mode and cyan for the shallow mode using $\epsilon = 10^{-4}$. Purple is for the deep mode and lime green for the shallow mode using $\epsilon = 10^{-4}$. All integrations used the linearized equations described in Section 5.6.1 and a reference state of $x_{sr} = 0.1$, $x_{dr} = 0.2$, $y_{sr} = y_s(0)$, $y_{dr} = y_d(0)$. Shown in the same format as in Fig. 12.

determinant. The purpose of the present subsection is to make a linear expansion for a non-zero determinant. We do however constrain the reference states of interest by linearizing about the equilibrium values of the cloud work function so that $y_{sr} = y_{dr} = 0$.

The linearized equations for this situation read as follows.

$$\dot{x}'_s = x_{sr} y'_s \tag{161}$$
$$\dot{x}'_d = \mu x_{dr} y'_d \tag{162}$$
$$\dot{y}'_s = x_{sr} - \hat{\beta}_d x_{dr} + x'_s - \hat{\beta}_d x'_d \tag{163}$$
$$\dot{y}'_d = -x_{dr} + \hat{\beta}_s x_{sr} - x'_d + \hat{\beta}_s x'_s \tag{164}$$

Taking a time derivative of the last two equations and then using the first two to eliminate $\dot{x}'_s$ and $\dot{x}'_d$ we find that

$$\ddot{y}'_s - x_{sr} y'_s + \hat{\beta}_d \mu x_{dr} y'_d = 0 \tag{165}$$

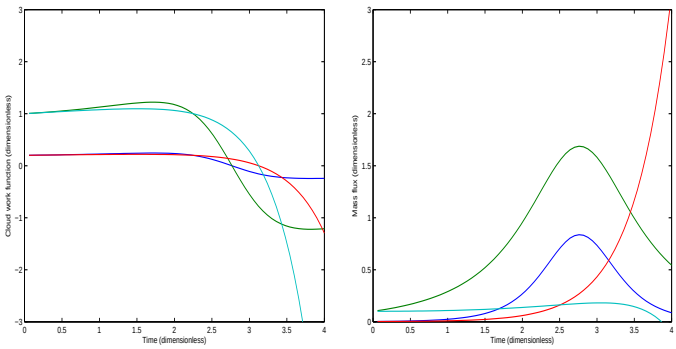


Figure 28: Numerical example solution for a linearized approximation of the unforced $p = 1$ system. The parameters are the default set described in Section 3.2, except for $\tau_d = 100$s, giving scaling factors of $A_{d0} = 100$ Jkg$^{-1}$, $A_{s0} = 1$ Jkg$^{-1}$, $M_{d0} = 5 \times 10^{-2}$ kgm$^{-2}$s$^{-1}$, $M_{s0} = 10^{-2}$ kgm$^{-2}$s$^{-1}$ and $\tau_s = 10^3$ s. The parameter $q = 0.5$. The initial conditions are $x_d(0) = 0.003$, $x_s(0) = 0.101$, $y_d(0) = 0.2$ and $y_s(0) = 1$. Blue is for the deep mode and green for the shallow mode using the fully nonlinear equations. Red is for the deep mode and cyan for the shallow mode using the linearized equations described in Section 5.6.1 and a reference state of $x_{sr} = 0.1$, $x_{dr} = 0.001$, $y_{sr} = 1$ and $y_{dr} = 0.2$. Shown in the same format as in Fig. 11.

$$\ddot{y}'_d + \mu x_{dr} y'_d - \hat{\beta}_s x_{sr} y'_s = 0 \tag{166}$$

It is then straightforward to obtain the eigenvalue equation

$$(\sigma^2 - x_{sr})(\sigma^2 + \mu x_{dr}) + \mu \hat{\beta}_d \hat{\beta}_s x_{sr} x_{dr} = 0 \tag{167}$$

or

$$\sigma^4 + (\mu x_{dr} - x_{sr})\sigma^2 + (\hat{\beta}_s \hat{\beta}_d - 1)\mu x_{sr} x_{dr} = 0 \tag{168}$$

The solution may be written as

$$\sigma^2 = \frac{\sigma_0^2}{2}\left(1 \pm (1 - \lambda)^{1/2}\right) \tag{169}$$

where we have defined

$$\sigma_0^2 = x_{sr} - \mu x_{dr} \tag{170}$$

$$\lambda = \frac{4(\hat{\beta}_s \hat{\beta}_d - 1)\mu x_{sr} x_{dr}}{\sigma_0^4} \tag{171}$$

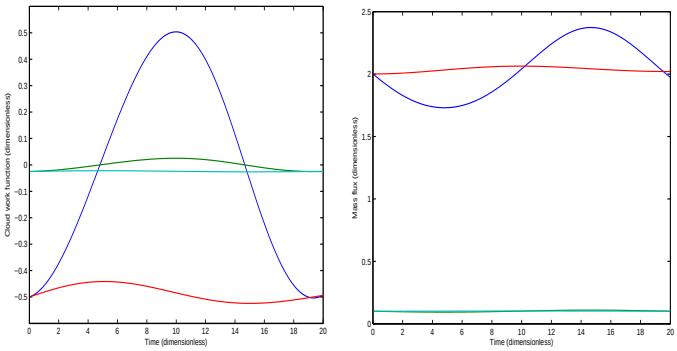


Figure 29: Numerical example solution for a linearized approximation of the unforced $p = 1$ system. The parameters are the default set described in Section 3.2, except for $\tau_d = 10^4$s, giving scaling factors of $A_{d0} = 1$ Jkg$^{-1}$, $A_{s0} = 1$ Jkg$^{-1}$, $M_{d0} = 5 \times 10^{-4}$ kgm$^{-2}$s$^{-1}$, $M_{s0} = 10^{-2}$ kgm$^{-2}$s$^{-1}$ and $\tau_s = 10^3$ s. The parameter $q = 0.5$. The initial conditions are $x_d(0) = 2.001$, $x_s(0) = 0.101$, $y_d(0) = -0.5$ and $y_s(0) = -0.025$. Blue is for the deep mode and green for the shallow mode using the fully nonlinear equations. Red is for the deep mode and cyan for the shallow mode using the linearized equations described in Section 5.6.1 and a reference state of $x_{sr} = 0.1$, $x_{dr} = 2$, $y_{sr} = -0.025$ and $y_{dr} = -0.5$. Shown in the same format as in Fig. 11.

The behaviour depends on the initial mass flux difference between shallow and deep convection, as measured by $\sigma_0^2$, and on the departure from a vanishing determinant, as measured by $\lambda$.

If $\lambda \leq 1$ then $\sigma^2$ is purely real and is either positive or negative in accordance with the sign of $\sigma_0^2$. Thus, there are purely oscillatory modes for $\sigma_0^2 < 0$ or both growing and decaying modes for $\sigma_0^2 > 0$. The other possibility is that $\lambda > 1$ and so $\sigma^2$ is complex. In that case there are both decay and growing oscillatory modes regardless of the sign of $\sigma_0^2$.

Most of these cases contain a growing mode indicating that there are no stable values of the mass flux when the coupled $p = 1$ system is started from the equilibrium values of the cloud work function. A numerical example is shown in Fig. 30. However, an exception occurs for $\sigma_0^2 < 0$ and $\lambda \leq 1$ in which case a linear perturbation produces a periodic solution, although this is no longer true in a fully nonlinear regime. An example solution for this regime is given in Fig. 31 and shows that convective activity is dissipated

away in the nonlinear regime, but that the system continues to oscillate in the linear approximation. The approximation breaks down relatively quickly in this case, at $t \sim 0.5\tau_s$.

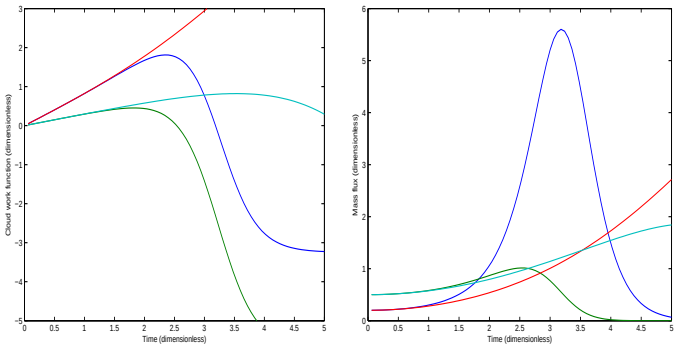


Figure 30: Solution for the unforced $p = 1$ system with finite determinant. The parameters are the default set described in Section 3.2, with the exception of $\beta_d = 0.2$ Jm$^2$kg$^{-2}$, giving scaling factors of $A_{d0} = 10$ Jkg$^{-1}$, $A_{s0} = 1$ Jkg$^{-1}$, $M_{d0} = 5 \times 10^{-3}$ kgm$^{-2}$s$^{-1}$, $M_{s0} = 10^{-2}$ kgm$^{-2}$s$^{-1}$ and $\tau_s = \tau_d = 10^3$ s. The initial conditions are $x_d(0) = 0.201$, $x_s(0) = 0.501$, $y_d(0) = 0$ and $y_s(0) = 0$. The parameters $\sigma_0^2 = 0.3$ and $\lambda = 4.4$. Blue is for the deep mode and green for the shallow mode using the fully nonlinear equations. Red is for the deep mode and cyan for the shallow mode using the linearized equations described in Section 5.7 and a reference state of $x_{sr} = 0.5$, $x_{dr} = 0.2$, $y_{sr} = y_{dr} = 0$. Shown in the same format as in Fig. 11.

## 5.8 Summary of results for the $p = 1$ system

The system of Eqs. 93 and 94 arises from Arakawa and Schubert's (1974) energy cycle description for a system with two types of convection, along with Yano and Plant's (2012a) linear assumption for the relationship between convective kinetic energy and cloud–base mass flux. All of the parameters in those equations are assumed to be positive in accordance with the arguments presented in Section 2.

The main points arising from our analysis of the system are that:

- The stability of the unforced shallow system in isolation depends on the initial conditions (Section 5.1), specifically the combination $r_s^2 \equiv$

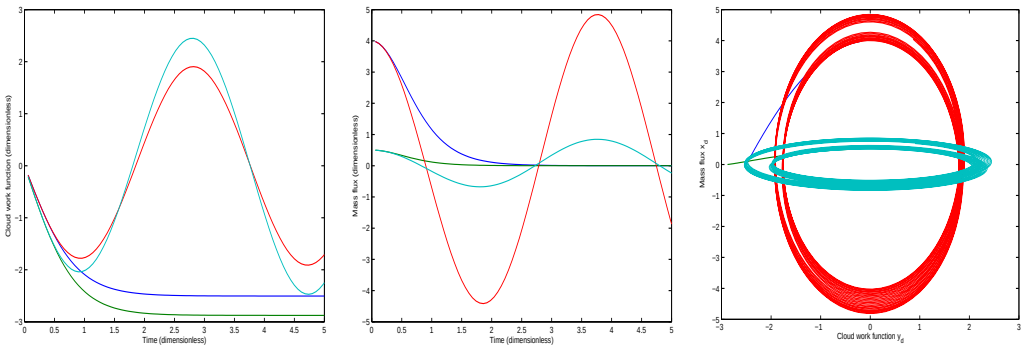

Figure 31: Solution for the unforced $p = 1$ system with finite determinant. The parameters are the default set described in Section 3.2, with the exception of $\beta_d = 0.2$ $\mathrm{Jm^2kg^{-2}}$, giving scaling factors of $A_{d0} = 10$ $\mathrm{Jkg^{-1}}$, $A_{s0} = 1$ $\mathrm{Jkg^{-1}}$, $M_{d0} = 5 \times 10^{-3}$ $\mathrm{kgm^{-2}s^{-1}}$, $M_{s0} = 10^{-2}$ $\mathrm{kgm^{-2}s^{-1}}$ and $\tau_s = \tau_d = 10^3$ s. The initial conditions are $x_d(0) = 4.001$, $x_s(0) = 0.501$, $y_d(0) = 0$ and $y_s(0) = 0$. The parameters $\sigma_0^2 = -3.5$ and $\lambda = 0.65$. Blue is for the deep mode and green for the shallow mode using the fully nonlinear equations. Red is for the deep mode and cyan for the shallow mode using the linearized equations described in Section 5.7 and a reference state of $x_{sr} = 0.5$, $x_{dr} = 4$, $y_{sr} = y_{dr} = 0$. Shown in the same format as in Fig. 12. Dashed curves are linear solutions.

$y_s(0)^2 - 2x_s(0)$. For $r_s^2 < 0$ the system explodes, for $r_s^2 = 0$ it either becomes infinite at the finite time $t = 2\tau_s/y_s(0)$ (if $y_s(0) > 0$) or else all convection is damped out (if $y_s(0) < 0$), and for $r_s^2 > 0$ then all convection is always damped out. Thus, in contrast to the $p = 2$ system, isolated shallow convection is not necessarily explosive but may decay if the initial mass flux is not too strong.

- The unforced deep system in isolation has vanishing convective activity (Section 5.2), regardless of the initial conditions. Thus, it behaves qualitatively like the $p = 2$ system.

- The coupled system may be unstable, damping or neutral according to the parameter settings and the initial conditions. It may also exhibit periodicity. As for the $p = 2$ system, solutions of particular interest are those for which the destablizing and stabilizing tendencies of shallow and deep convection respectively are balanced. Such solutions may still

vary in time but they do not persistently grow or decay. A necessary condition for such a solution is that the determinant of the interaction matric $\mathcal{K}_{ij}$ should vanish (Section 4.4.1; Eq. 32).

- The nonlinear $p = 1$ system also has a further requirement on the initial conditions (Section 5.4; Eq. 127), which we call the initial periodicity condition. The requirement is that $r_c = y_s(0) - \hat{\beta}_d y_d(0) = 0$. If the determinant vanishes but $r_c \neq 0$ then the coupled system aproaches a single-mode system as $t \to \infty$ with shallow (deep) convection dominant for $r_c$ positive (negative).

- Assuming a vanishing determinant and initial periodicity:

  - The shallow and deep convective mass fluxes are linked through a power relationship with power $q = (\beta_d \alpha_d)/(\gamma_d \alpha_s)$ as given in Eq. 132 of Section 5.5. The qualitative behaviour of the two–mode system is controlled by this power $q$,

    * For $q > 1$ (Section 5.5.1) either all activity dies out or else the system explodes. Which of these possibilities occurs can be determined from the initial mass flux, which must be smaller than a threshold value for decay. The threshold for the deep convective mass flux is stated in Eq. 138.
    * For $q = 1$ (Section 5.5.2), the deep and shallow mass fluxes are proportional and again either all activity dies out or else the system explodes. Which of these possibilities occurs can be determined by comparing the initial values of mass flux for deep and shallow convection. Decay occurs if the deep convective mass flux is sufficiently strong that $x_d(0) > \hat{\beta}_s x_s(0)$.
    * For $q < 1$ (Section 5.5.3), the solution is periodic regardless of any further considerations of the initial conditions.

  - We considered a linearization of the equations in order to consider the system with vanishing determinant but with a small departure from initial periodicity. Specifically, we expanded about a reference state that respects initial periodicity (Section 5.6.1).

    * Departures from a reference state of zero mass flux produce growth if the reference cloud work functions are larger than their equilibrium values and decay otherwise (Section 5.6.2).
    * Departures from the equilibrium values of the cloud work functions grow for $q > 1$ and are oscillatory for $q < 1$ (Section 5.6.3).

    - Numerically the linearized solutions provide a good description for $\mu \sim 1$ but perform poorly for $\mu \gg 1$ and $\mu \ll 1$ (Section 5.6.4) in which one mode dominates and non-linear effects are important.
  - We also considered a linearization of the equations in order to explore the case of a non-vanishing determinant with a small departure from equilibrium values of the cloud work functions (Section 5.7). In that case most parameter settings and initial conditions lead to a growing mode increasing the linear departure from the cloud work function equilibrium. However, the departure may be neutral, producing a periodic solution of the linearized equations, if $\sigma_0^2 < 0$ and $\lambda \leq 1$ where $\sigma_0$ and $\lambda$ are defined by Eqs. 170 and 171 respectively.

To summarize the summary, for most configurations of the $p = 1$ system convection will either decay or explode and the rules above enable us to determine which of these will occur for any given parameter settings and initial conditions. However, the system also supports a bounded periodic solution under the following conditions:

1. The matrix determinant must vanish, $\beta_d \beta_s = \gamma_d \gamma_s$.
2. The forcing must satisfy $F_s = \frac{\gamma_s}{\beta_s} F_d$ which of course includes the case of no forcing.
3. The initial conditions for the cloud work function must satisfy $A_s(0) - A_{s0} = \frac{\gamma_s}{\beta_s} (A_d(0) - A_{d0})$
4. The other parameters of the problem must respect the inequality $q < 1$.

# 6 Final remarks

A careful consideration of the behaviour of the two mode system has been presented in this report, and should be considered a last step before we move on to consider fully statistical aspects of the convective energy–cycle system with many convective modes. Understanding the basic behaviour of the two–mode system under interactions between shallow and deep convection is an indispensable starting point for the multi–mode system.

Although a full discussion of the implementation of the prognostic energy–cycle into a convection parameterization is beyond the scope of the present

report, the principle is clear. It is straightforward to implement the energy-cycle formulation into standard mass–flux based convection parameterizations (*cf.*, Arakawa and Schubert 1974), because the energy cycle can be consistently reproduced under this parameterization framework (*cf.*, Yano and Plant 2011, 2012a). A similar energy cycle has already been implemented into a spectral mass–flux parameterization by Pan and Randall (1998). However, they did not consider coupling between different convective modes. The inclusion of such couplings presents no formulational difficulties.

Another interesting possibility could be to exploit the above results as selection criteria for use alongside existing *equilibrium* shallow and deep convcetive parameterizations. Current models typically use somewhat ad hoc criteria for deciding whether to apply a shallow scheme or a deep scheme or possibily both. However, from the results presented above, we can always determine which of three situations arises in a coupled prognostic system:

1. the freely-running system with no external interactions (*i.e.*, no forcing) would decay to zero. In this situation, deep convective dynamics is dominant so we should make a call to the deep parameterization only.

2. the freely-running system with no external interactions (*i.e.*, no forcing) would explode. In this situation, shallow convective dynamics is dominant so we should make a call to the shallow parameterization only.

3. the freely-running system with no external interactions (*i.e.*, no forcing) is periodic. In this situation, shallow and deep convective dynamics are very tightly coupled together so we should make calls to both of the parameterizations.

# A Dimensional analysis and the functional relation, Eq. 5

A general functional relation 5 with $p \neq 2$ may at first sight be objected to on dimensional grounds. A dimensional analysis says that the only consistent manner for linking the kinetic energy density, $k$ (J/kg), and a characteristic velocity scale, $w_{\rm char}$, would be to set

$$k = \frac{1}{2} w_{\rm char}^2 \tag{172}$$

The purpose of this appendix is to show that this standard expression of dimensional analysis does not contradict with Eq. 5.

The convective kinetic energy, $K$, (which is vertically integrated) is given by

$$K = \int_{z_B}^{z_T} \sigma_c \frac{\rho}{2} w^2 dz \tag{173}$$

where $w$ is the vertical velocity in the convective updraft and where attention has been restricted to the vertical component of velocity only, as in Yano and Plant (2012a). All other notation is as defined in the main text. This quantity $K$ is to be compared with the cloud–base mass flux, which is defined by

$$M_b = \rho_b \sigma_b w_b. \tag{174}$$

In order to relate the vertically–integrated convective kinetic energy, $K$, with the convective energy density, $k$, we normalize the former by using the cloud–base values, $\sigma_b$ and $\rho_b$, and we measure its vertical scale by $h$. As a result,

$$K = \rho_b \sigma_b h k \int_0^1 \frac{\sigma}{\sigma_b} \frac{\rho}{\rho_b} \left( \frac{w}{w_{\rm char}} \right)^2 d(z/h) \tag{175}$$

The integral now depends on dimensionless vertical profiles only and we can denote its value as $2\zeta$, which is assumed to take a fixed value for some suitable choice of $w_{\rm char}$.

Hence we can write

$$K = \zeta \frac{w_{\rm char}^2 h M_B}{w_b} \tag{176}$$

Now we must address the issue of the characteristic velocity scale $w_{\rm char}$. It is immediately clear that the choice of this scale, and its dependence (if any) on the cloud-base mass flux will determine a suitable choice for $p$ in an equation of the form of Eq. 5. In other words $p = 2$ is *not demanded* by a priori by a dimensional analysis. A choice of $p$ indicated by dimensional analysis can only begin to be discussed after one has introduced and justified physical assumptions to obtain the velocity scale $w_{\rm char}$. Some specific examples are discussed below.

1. As a trivial example we could set $w_{\rm char} \sim L_v^{1/2}$ where $L_v$ is the latent heat of vaporization. It must be stressed do not believe this scaling to be physically appropriate but clearly the latent heat parameter $L_v$ is a relevant quantity for moist convection and on dimensional grounds alone this scaling cannot be held objectionable. In this case we might then choose $p = 1$ if we believe that $\zeta h / w_b$ can be treated as constant, or $p = 0$ if we believe that $\zeta h \sigma_b$ can be treated as constant.

2. A more reasonable possibility is to choose $w_{\rm char} = w_b$ so that $w_b$ is the only velocity scale involved. In that case $K \sim \sigma_b w_b^2 h$. This consistent with $p = 2$ in Eq. 5 if $\zeta h/\rho_b\sigma_b$ can be treated as constant for a given convection type. However, we argued in Plant and Yano (2012a) this cannot be strictly true, because numerical results show that $\sigma_b$ does indeed change with a change of $M_b$. In particular, if changes of $M_b$ are dominated by those in $\sigma_b$ rather than those in $w_b$ (which we argued was a better interpretation of the numerical results), then we may set $p = 1$ by treating $\zeta h w_b$ as constant. Thus, we see that apparent inconsistency of Eq. 5 with the dimensional analysis stems from the fact that nondimensional variables such as $\sigma_b$ may play a leading role.

3. Other scales for $w_{\rm char}$ have been proposed. For example, Grant and Brown (1999); Grant and Lock (2004) considered a velocity scale based on CAPE,

$$w_{\rm cp} = \sqrt{\rm CAPE} \tag{177}$$

and a convective velocity scale $w^*$ defined by

$$w^* = \left( {\rm CAPE} \frac{M_b}{\rho_b} h \right)^{1/3} . \tag{178}$$

This latter scale is obtained by equating the generation and dissipation rates of turbulent kinetic energy and scaling these as ${\rm CAPE}\, M_b$ and $\rho_b w^{*3}/h$ respectively. Grant and Brown (1999) in their Figure 4 showed results for scaling the convective-core contribution to kinetic energy from their simulations for shallow convection. The results show that $w_{\rm char} = w_{\rm cp}$ and $w_{\rm char} = w^*$ are both effective at collapsing the curves, although the latter case is perhaps a little better and is the one that is consistent with their physical arguments.

If we take $w_{\rm char} = w_{\rm cp}$ then this would suggest taking $p = 1$ if $\zeta\, {\rm CAPE}\, h/w_b$ is treated as constant or else $p = 0$ if $\zeta\, {\rm CAPE}\, h\rho_b\sigma_b$ is treated as constant.

On the other hand, if we take $w_{\rm char} = w^*$ then this would suggest taking $p = 5/3$ if $({\rm CAPE}\, h/\rho_b)^{2/3} h(\zeta/w_b)$ can be treated as constant or $p = 2/3$ if $({\rm CAPE}\, h/\rho_b)^{2/3} h\zeta\rho_b\sigma_b$ can be treated as constant. Of course, it must be remembered that the velocity scale $w^*$ is based on a different assumption by Grant and Brown (1999) for the form of the dissipation rate compared to that in the main text.

## References

Arakawa, A., and W. H. Schubert, 1974: Interaction of a cumulus cloud ensemble with the large-scale environment, Part I. *J. Atmos. Sci.*, **31**, 674–701.

Benedict, J. J., and D. A. Randall, 2007: Observed characteristics of the MJO relative to maximum rainfall. *J. Atmos. Sci.*, **64**, 2332–2354.

Betts, A. K., 1997: Trade cumulus: observations and modelling. In: *The Physics and Parameterization of Moist Atmospheric Convection*, Kluwer Academic Publ., 99–126.

Deadorff, J. W., 1980: Cloud top entrainment instability. *J. Atmos. Sci.*, **37**, 1211–1213.

Emanuel, K. A., and M. Bister, 1996: Moist convective velocity and buoyancy scales. *J. Atmos. Sci.*, **53**, 3276–3285.

Emanuel, K. A., J. D. Neelin, and C. S. Bretherton, 1994: On large–scale circulation in convective atmospheres. *Quart. J. Roy. Meteor. Soc.*, **120**, 1111–1143.

Grant, A. L. M. and A. R. Brown, 1999: A similarity hypothesis for shallow-cumulus transports. *Quart. J. Roy. Meteor. Soc.*, **125**, 1913–1936.

Grant, A. L. M. and A. P. Lock, 2004: The turbulent kinetic energy budget for shallow cumulus convection. *Quart. J. Roy. Meteor. Soc.*, **130**, 401–422.

Guichard F., J. C. Petch, J. L. Redelsperger, P. Bechtold, J.–P. Chaboureau, S. Cheinet, W. Grabowski, H. Grenier, C. G. Jones, M. Kohler, J.–M. Piriou, R. Tailleux, and M. Tomasini, 2004: Modelling the diurnal cycle of deep precipitating convection over land with cloud-resolving models and single-column models. *Quart. J. Roy. Meteor. Soc.*, **604**, 3139–3172.

Hohenegger, C., and C. S. Bretherton, 2011: Simulating deep convection with a shallow convection scheme. *Atmos. Chem. Phys.*, **11**, 8385–8430.

Holtslag, A. A. M., and B. A. Boville, 1993: Local versus nonlocal boundary–layer diffusion in a global climate model. *J. Climate*, **6**, 1825–1842.

Houze, R. A., Jr., and A. K. Betts, 1981: Convection in GATE, *Rev. Geophys. Space Phys.*, **19**, 541-576.

Johnson, R. H., Rickenbach, T. M., Rutledge, S. A., Ciesielski, P. E., and Schubert, W. H., 1999: Trimodal characteristics of tropical convection. *J. Climate*, **12**, 2397–2418.

Köller, M., M. Ahlgrimm, and A. Beljaars, 2011: Unified treatment of dry convective and stratocumulus–topped boundary layers in the ECMWF model. *Quart. J. Roy. Meteor. Soc.*, **137**, 43–57.

Lock, A. P., 1998: The parameterization of entrainment in cloudy boundary layers. *Quart. J. Roy. Meteor. Soc.*, **124**, 2729–2753.

Lock, A. P., A. R. Brown, M. R. Bush, G. M. Martin, and R. N. B. Smith, 2000: A new boundary layer mixing scheme. Part I: Scheme description and single–column model tests. *Mon. Wea. Rev.*, **128**, 3187–3199.

Mapes, B. E., and R. Meale, 2011: Parameterizing convective organization to escape the entrainment dilemma. *J. Adv. Model Earth System*, **3**, doi:10.1029/2011MS000042.

Moeng, C.–H., 1998: Stratocumulus–topped atmospheric planetary boundary layer. In: *Buoyant convection is Geophysical Flows*, E. J. Plate, E. E. Fedorovich, D. X. Viegas, and J. C. Wyngaard, Eds., Kulwer Academic Publ., 421–440.

Neggers, R., M. Köller, and A. Beljaars, 2009: A dual mass flux framework for boundary–layer convection. Part I: Transport. *J. Atmos. Sci.*, **66**, 1465–1487.

Pan, D.-M., and D. A. Randall, 1998: A cumulus parameterization with prognostic closure, *Quart. J. Roy. Meteor. Soc.*, **124**, 949–981.

Parodi, A., and K. Emanuel, 2009: A theory for buoyancy and velocity scales in deep moist convection. *J. Atmos. Sci.*, **66**, 3449–3463.

Parsons, D. B., K. Yoneyama, K., and J.–L. Redelsperger, 2000: The evolution of the tropical western Pacific atmosphere–ocean system following the arrival of a dry intrusion. *Quart. J. Roy. Meteor. Soc.*, **126**, 517–548.

Randall, D. A., 1980: Conditional instability of the first kind upside down. *J. Atmos. Sci.*, **37**, 125–130.

Randall, D. A., and D.-M. Pan, 1993: Implementation of the Arakawa-Schubert cumulus parameterization with a prognostic closure. In: *The Representation of Cumulus Convection in Numerical Models*, K. A. Emanuel and D. J. Raymond (Eds.), Meteorological Monographs **46**, Amer. Meteor. Soc., 137–144.

Riehl, H., C. Yeh, J. S. Malkus, and N. E. LaSeur, 1951: The north–east trade of the Pacific Ocean. *Quart. J. Roy. Meteor. Soc.*, **77**, 598–626.

Redelsperger, J.–L., 1997: The mesoscale organization of deep convection. In: *The Physics and Parameterization of Moist Atmospheric Convection*, R. K. Smith (Ed.), Kluwer Academic Publ., 59–98.

Riehl, H., and J. S. Malkus, 1958: On the heat balance in the equatorial trough

zone. *Geophysica*, **6**, 503–538.

Shutts, G. J., and M. E. B. Gray, 1999: Numerical simulations of convective equilibrium under prescribed forcing. *Quart. J. Roy. Meteor. Soc.*, **125**, 2767–2787.

Stevens, B., 2005: Atmospheric moist convection. *Ann. Rev. Earth Planet. Sci.*, **33**, 605–643.

Tiedtke, M., 1989: A comprehensive mass flux scheme of cumulus parameterization in large–scale models. *Mon. Wea. Rev.*, **117**, 1779–1800.

Tung, W. W., C. Lin, B. Chen, M. Yanai, and A. Arakawa, 1999: Basic mode of cumulus heating and drying observed during TOGA–COARE IOP. *Geophys. Res. Lett.*, **26**, 117–120.

Wyant, M. C., C. S. Bretherton, A. Chlond, B. M. Griffin, H. Kitagawa, C.–L. Lappen, V. E. Larson, A. Lock, S. Park, S. R. de Roode, J. Uchida, M. Zhao, A. S. Ackerman, 2007: A single–column model intercomparison of a heavily drizzling stratocumulus–topped boundary layer. *J. Geophys. Res.*, **112**, D24204, doi:10.1029/2007JD008536.

Yano, J.–I., and R. S. Plant, 2011: Introduction to Statistical Cumulus Dynamics. *COST ES0905 Document*, available at http://convection.zmaw.de/fileadmin/user_upload/convection/Convection/ms1.pdf

Yano, J.-I., and R. S. Plant, 2012a: Finite departure from convective quasi-equilibrium: Periodic cycle and discharge-recharge mechanism. *Quart. J. Roy. Meteor. Soc.*, **138**, 626–637.

Yano, J.-I., and R. S. Plant 2012b: Interactions between shallow and deep convection under a finite departure from convective quasi–equilibrium. *J. Atmos. Sci.*, accepted.